Optically Inaccessible Flow Visualization using Positron Emission Tomography

TECHNICAL BRIEFING

JEREMY BRUGGEMANN

MAY 3RD, 2018

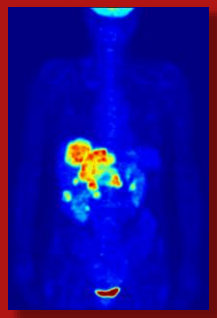

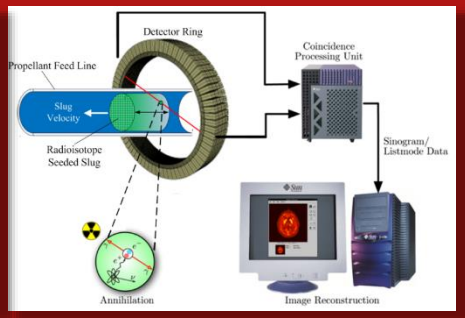

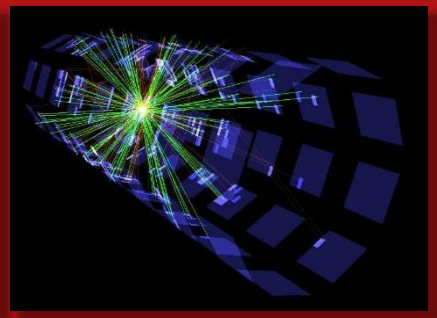

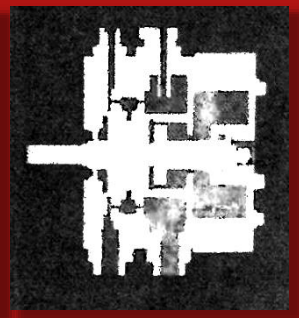

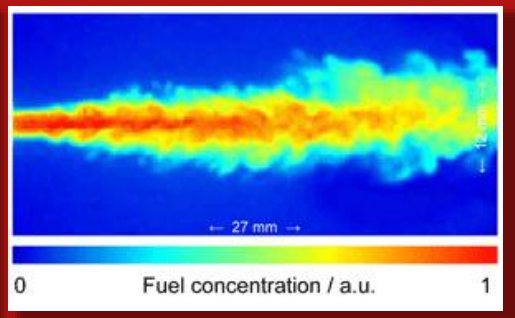

Outline

- Section 1 - Introduction
- Section 2 - Methodology Overview
- Section 3 – Computational Fluid Dynamics – Steady State Turbulent Flow
- Section 4 – Computational Fluid Dynamics – Transient Scalar Transport Simulation
- Section 5 – GEANT4 Application for Tomographic Emission (GATE) Simulation
- Section 6 – Image Reconstruction – Software for Tomographic Image Reconstruction (STIR)
- Section 7 – Path Forward

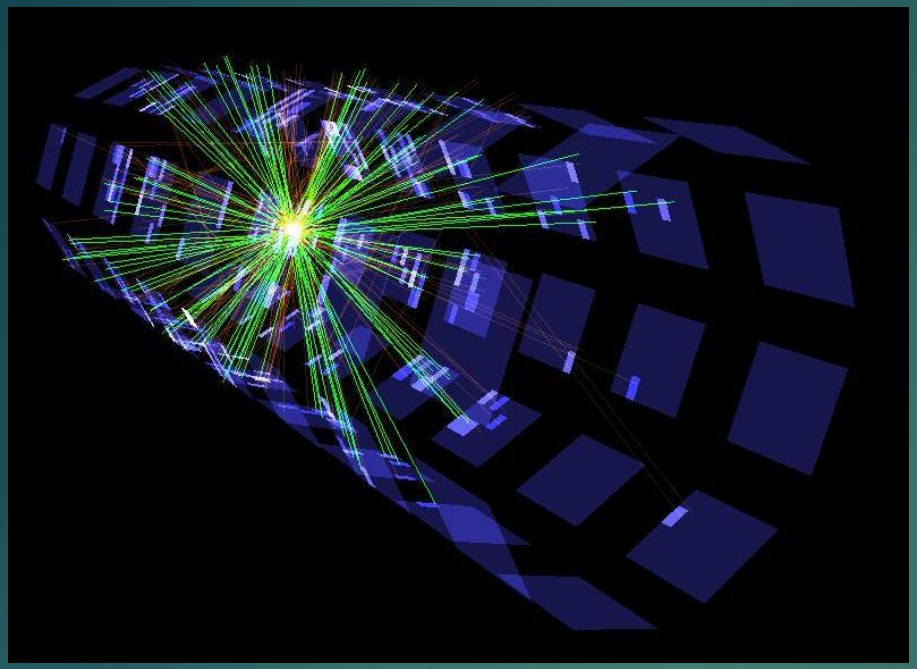

INTRODUCTION

MOTIVATION
CONCEPT DESCRIPTION
ADVANTAGES
LITERATURE SURVEY
OBJECTIVES

Motivation

- Flow visualization of optically inaccessible flows is needed to characterize flow within as-built, integrated systems
- A Possible Solution: Positron Emission Tomography (PET)
  - Used widely in the medical field to non-intrusively visualize 3D fluid distributions in humans and small animals
  - Used to diagnose physiological processes
- PET Technology is becoming more relevant to applications in engineering field
  - Silicon Photo Multipliers (SiPMs)/ Avalanche Photo Diodes (APD) replaces traditional PMTs – increased signal to noise ratio
  - Lutetium Yttrium Oxyorthosilicate (LYSO) scintillation material replacing NaI scintillators
    - Shorter scintillation decay time – reduced dead time
    - Increased gamma-ray stopping power
    - Enables Time-of-Flight (TOF) reconstruction algorithm

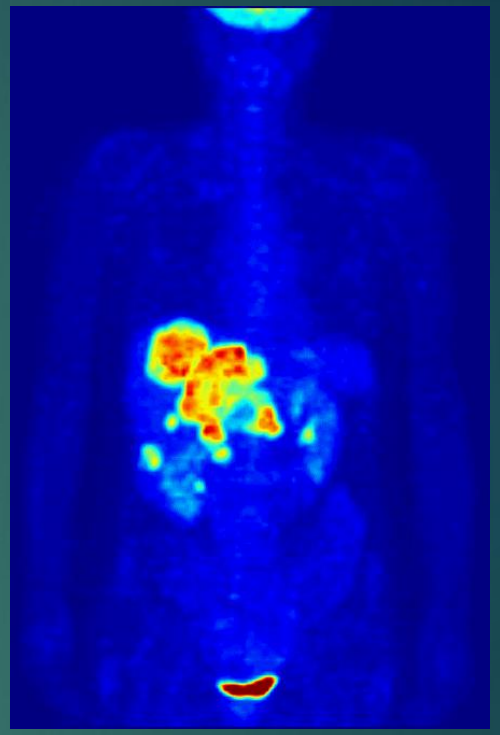

Whole-body PET scan using ^{18}F-FDG (Ref. 8)

2007

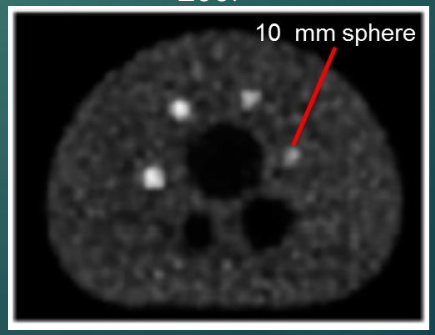

60 Sec Acquisition PET used to image 37 and 28 mm cold spheres, and 22, 17, 13, and 10 mm hot spheres in torso phantom. NOTE: SiPMs not used. (Source: Ref. 3)

PET Physics & Instrumentation

- Beta+ Decay
  - Unstable radioisotopes emit positrons with initial kinetic energy
  - Kinetic energy reduced through interaction with surrounding media until sufficiently low to annihilate with electrons
  - Produces two nearly collinear 511 keV gamma-rays propagating in opposite directions
- PET Detectors
  - Gamma-rays interact (primarily Compton scatter) with scintillating crystals emitting optical photons
  - Optical photons are detected by PMTs/SiPMs
- Single detections are processed to identify coincident detections within specified time window
- Coincident detections = Line of Response (LOR) between triggered detectors
- Multiple LORs and time-of-flight (TOF) data used to reconstruct radioisotope distribution

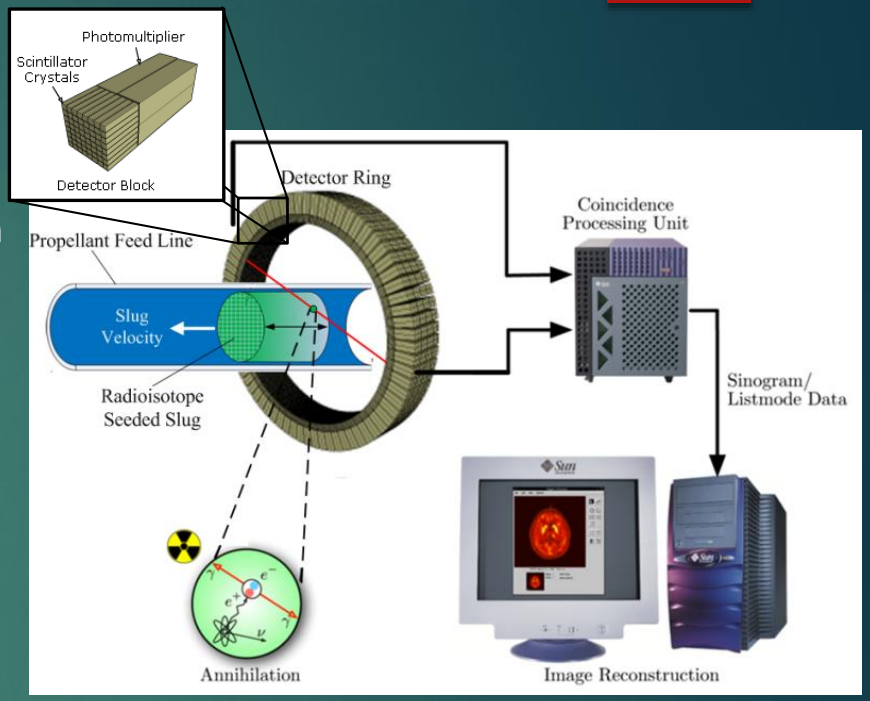

Conceptual schematic of PET applied to visualizing flow in a pipe (Modified from Ref. 8)

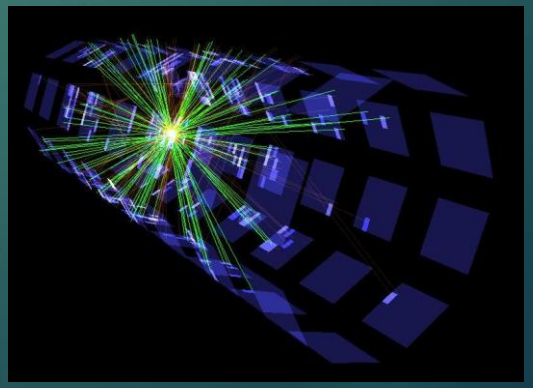

Measured LORs for 3 ml slug of F-18/water solution in Modular Unit at Positron Imaging Centre of Univ. of Birmingham, UK

Concept Description

- General flow visualization concept description
  - Inject Beta+ emitting radioisotopes "In-solution" into flow of interest
    - Utilize radioisotopes of bulk media or compatible constituent
    - Oxygen-15 for oxidizer systems – 2 min. half-life
    - Carbon-11 for hydrocarbon based fuel systems – 20.3 min. half-life
    - Krypton-79 for Krypton based electric propulsion systems – 35 hr. half-life
    - Etc. – many to choose from
  - Utilize PET system to detect back-to-back gamma ray (511 keV) emissions resulting from the decay process
  - Utilize image reconstruction algorithms to generate images of the 3D radioisotope distribution as it traverses the flow of interest
  - Attenuation mapping applied to reconstruction algorithm provided by 3D CAD models for increased resolution.

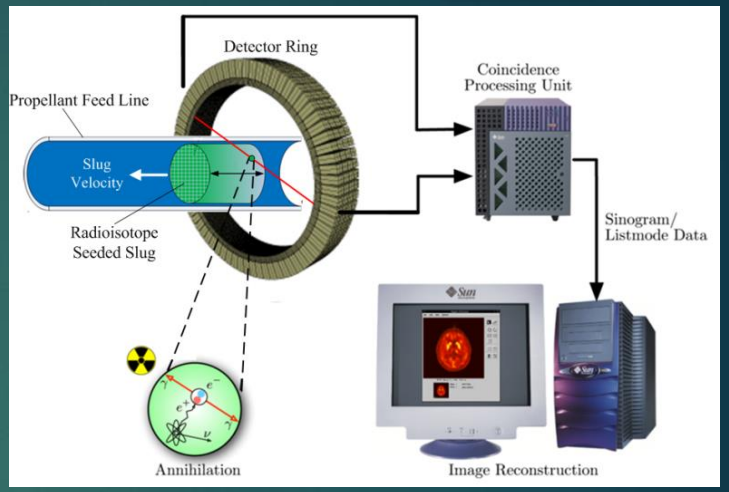

Conceptual schematic of PET applied to visualizing flow in a pipe (Modified from Ref. 8)

State-of-the-art desktop microPET system likely candidate for pipe flow visualization.

Advantages

- Benefits of flow/fluid distribution visualization of optically inaccessible flow fields with PET Technology
  - Gamma rays are highly energetic (511 keV) enabling penetration of fluid containment materials
  - Fluid dynamics of fully integrated systems can be characterized
  - Using radioisotope of the bulk media preserves thermochemical properties during visualization process
  - Radiobiological hazards mitigated due to relatively short radioisotope half lives, e.g. 2 minutes for O-15
  - 3D CAD models of engineering system can be superimposed on 3D radioisotope distribution data for high fidelity visualization

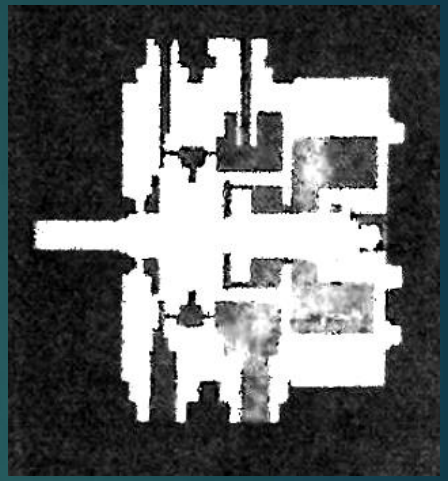

1988 - Bearing rig oil injection visualization – 3D CAD model superimposed (Source: Ref.4)

Literature Survey

- PET application in the Engineering Field
  - 1988 – Visualization of faulty oil injection in bearing rig using Multi-wire Proportional Counter.[Ref. 1]
  - 2008 – Visualization of pharmaceutical mixing in steel drums[Ref. 2]
- Early 1990's to present - Positron Emission Particle Tracking (PEPT) used to characterize particle 3D dynamics in mechanical systems – pioneered at the Positron Imaging Centre (PIC)
  - Variation of traditional PET as only, up to, a few particles are tracked at one time
  - Sub-millimeter sized particles tracked to within 1.5 to 2.0 mm for velocities up to 100 m/s. [Ref. 2]
    - Lower velocities enable increased precision
  - Draw back: characterizing flows requires a significant number of particles.

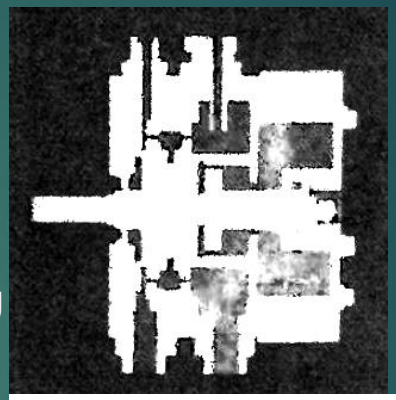

Bearing rig oil injection visualization (left) - 60 minute acquisition (Source: Ref.4)

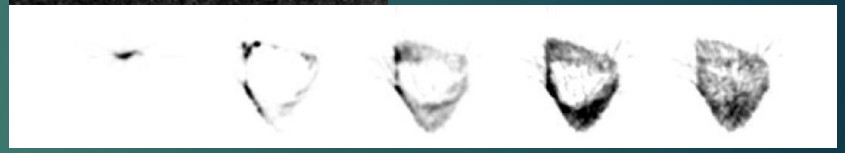

Visualization of pharmaceuticals progressively mixing in 0.3 m diameter steel drums (above) – 20 minute acquisition. (Source: Ref. 5)

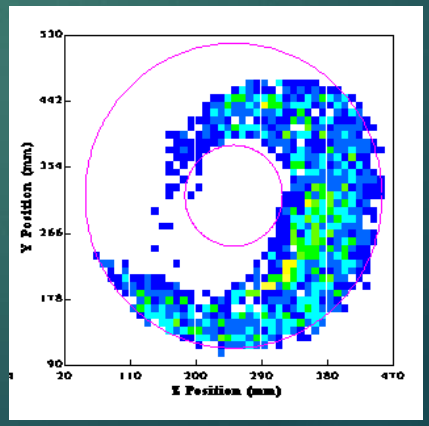

Particle residence times of particle tracked in mechanical mixing system. (Source: Ref. 2)

Literature Survey (cont.)

- Alternate Optically Inaccessible Flow Visualization Techniques
  - Neutron Radiography: Ref. 1
    - 1988 application of Neutron Radiography led to 2D mapping of oil distribution in Rolls Royce Gem Engine
    - Aeration found in return line causing engine oil overfilling and leaking
    - Limited to 2D with occlusion caused by oil build up on engine walls in the foreground
  - Ultrafast Electron Beam X-ray Computed Tomography: Ref. 3
    - 2012 application using X-rays to visualize multiphase flow through pipelines with liquid velocities of up to 1.4 m/s
    - Tests were performed with gas inlet pressures of 2.5 bar
    - Limited to low pressure applications due to order of magnitude larger attenuation coefficient

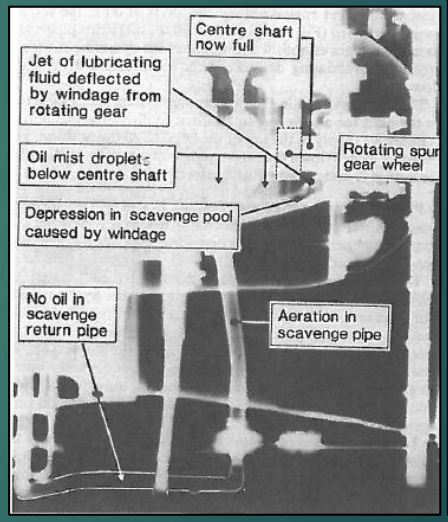

Rolls Royce Gem Engine oil injection visualization – snap shot of real time acquisition. (Source: Ref.1)

Virtual three dimensional plots of two phase flow obtained using X-ray CT. (Source: Reference 3)

Objective

- Overall objective: Parametrically bound the applicable flow fields that can be sufficiently visualized using a modern PET systems
- PhD Research Objectives as stated in the IDOC Proposal
  - Utilize computational simulation tools to simulate a PET detectors response to a transient distribution of Flourine-18 radioisotope solution flowing through an orifice plate with diametric ratio of 0.5 for various Reynolds Numbers.
  - Utilize simulation results to assess the ability of a modern microPET system to resolve the following flow features:
    - Short time scale features: Vena contracta & reattachment point downstream of the orifice
    - Long time scale features: orifice axial location, orifice diameter

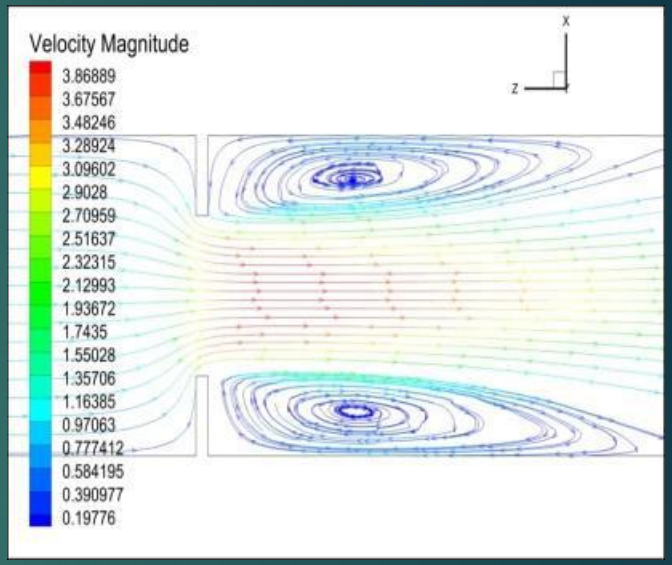

Orifice Flow with β=0.5 and Re = 15000 showing primary flow and secondary, separated flow.

Methodology Overview

SECTION 2

Methodology - Work Flow

CFD Simulation Software

- Steady state turbulent flow solution
- Transient "scalar" transport

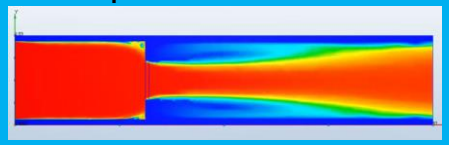

GATE Simulation Software

- Radioisotope decay & e^+ annihilation process
- Gamma Ray emission and attenuation
- PET detector system response

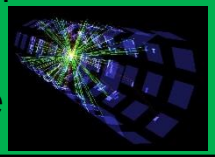

ROOT Analysis Software

- Coincident detection projections

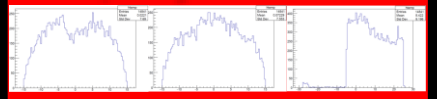

Software for Tomographic Image Reconstruction (STIR)

- Iterative and Analytic image reconstruction

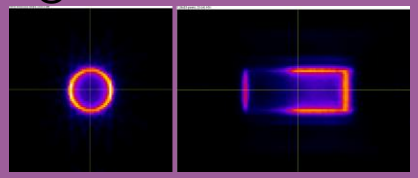

Comparison Analysis

- Long timescale features: Orifice parameters
- Short timescale features: vena contracta, reattachment points

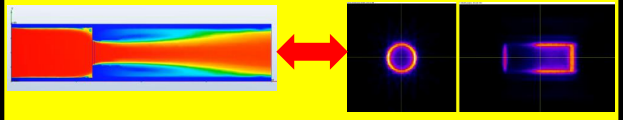

Methodology – Key CFD Parameters

- Key CFD Parameters
  - Flow Reynolds number – nondimensional parameter accounting for fluid velocity (V), flow characteristic length (pipe diameter (D)), fluid density (ρ), and fluid viscosity(μ)

$$Re = \frac{\rho V D}{\mu}$$

    - Reynolds parameters held constant: $\rho = 998\,{}^{kg}/_{m^3}$, $D = 52.6\,mm$, and $\mu = 8.9 \times 10^{-4}\,{}^{N \cdot s}/_{m^2}$
    - V varied to produce Reynolds numbers: ~67,000, 87,000, 136,000, and 183,000
      - Corresponds to cases tested by Bates (1981)
      - $Re = 67{,}000$ corresponds to case tested by Ahmed (2012)
  - Radioisotope fluid dynamic parameter
    - Radioisotope: Flourine-18 (F-18)
    - Diffusivity: $D = 1.89 \times 10^{-5}\,{}^{cm^2}/_{s}$
    - Inlet concentration: specified as activity concentration based on required activity in the scanner field of view – see next slide

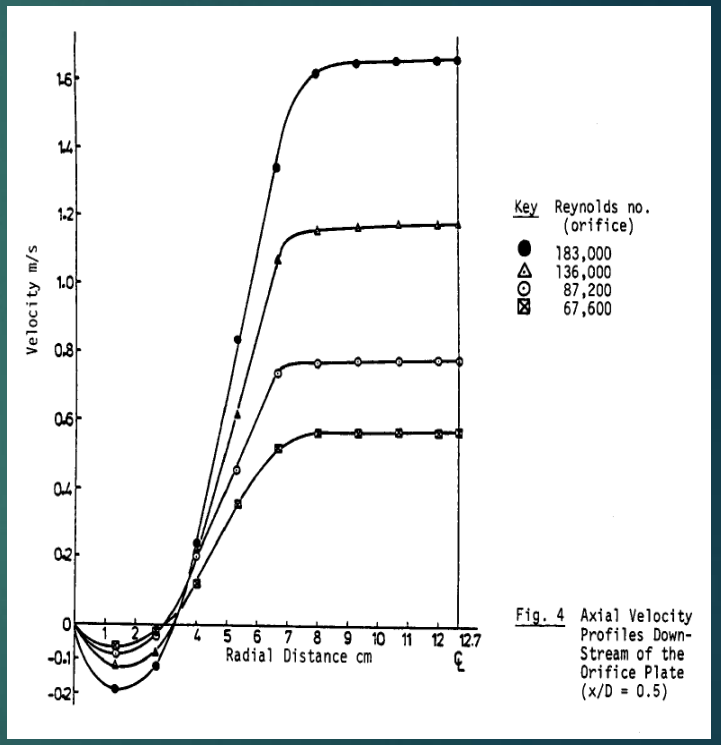

Fig. 4 Axial Velocity Profiles Down-Stream of the Orifice Plate (x/D = 0.5)

Methodology – Key Physics Parameters

- Key Physics Parameters
  - Overall PET system performance
    - The Siemens Inveon PET system has been modelled in GATE and will be used in all test cases.
    - Subsystem/Hardware Parameters are selected to represent the systems actual configuration – i.e. energy thresholds, dead time losses, Field of View, Etc.
  - Gamma ray attenuation due to fluid and fluid containment – configurationally specific
    - Held constant for all test cases as the same pipe and orifice geometry will not be changed
  - Radioisotope physics parameters
    - Decay half-life: ~110 min. – sufficiently long compared to time scale of simulation (~10 sec) to neglect changes in concentrations due to radioactive decay.
    - Activity concentration: Based on required activity in the scanner field of view to meet peak NECR count rate. – constant across each case

$$C_A = \frac{A_{maxNECR}}{V_{FOV}} = 0.36\ {}^{MBq}/_{cm^3}$$

Siemens Inveon PET System

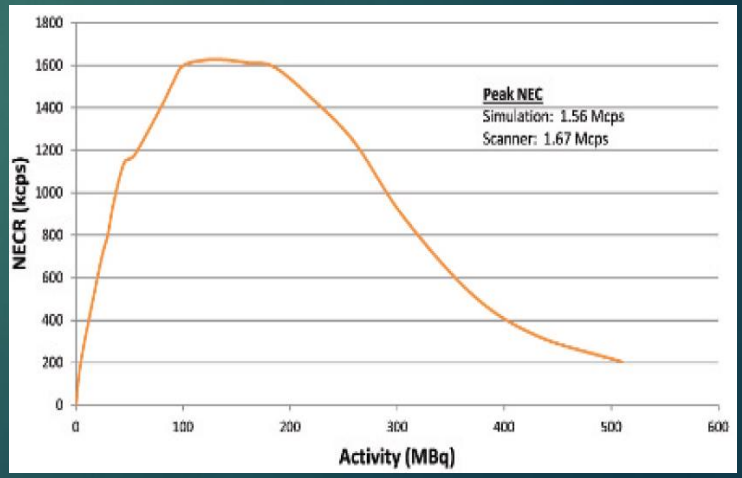

Siemens Inveon NECR performance curve

Computational Fluid Dynamics – Steady State Turbulent Flow Solution

SECTION 3

Computational Domain Definition

- Primary Objective: Define a Computational domain and mesh that is optimized for reasonable CFD accuracy and GATE simulation computational demand.
- Pipe specification:
  - 2 in. ANSI schedule 40 steel pipe
    - Diameter: 52.6 mm
    - Wall thickness: 3.81 mm (nominal)
- Orifice specification
  - Square edge with 30° downstream bevel – British industry standard to match Bates (1981) experiment configuration.
  - Pipe-Orifice Diameter ratio: $\beta = 0.5$
- Bulk Fluid Specification: Water @ 21 °C (70 °F)

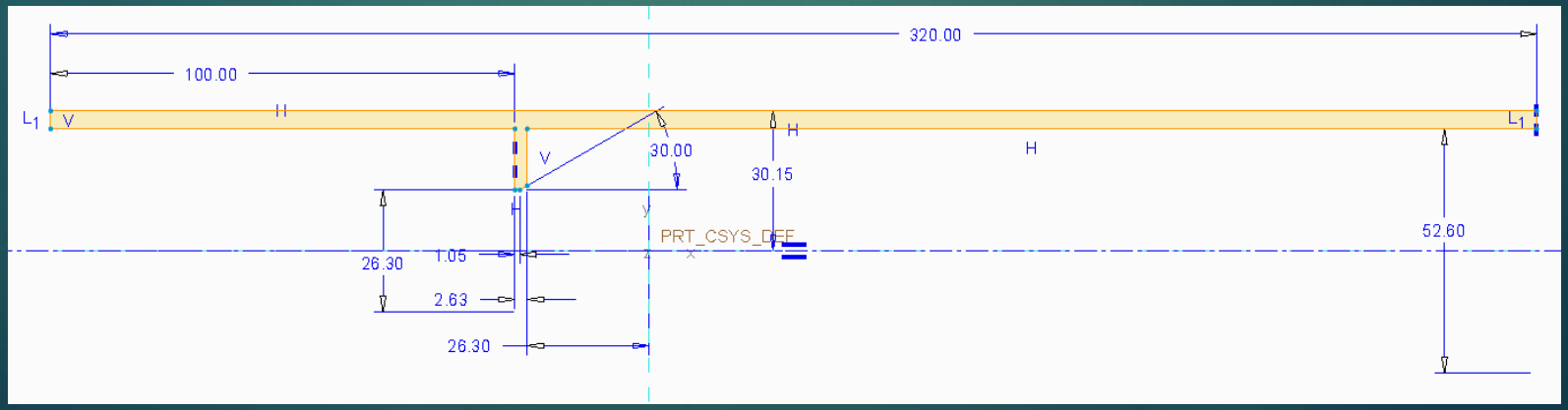

Boundary Conditions

- Turbulent Steady State – Re = 67,000
  - Inlet Mean Velocity = 0.4 m/s (fully developed flow profile)
  - Outlet Pressure = 0 kPa
  - Walls = Non-slip

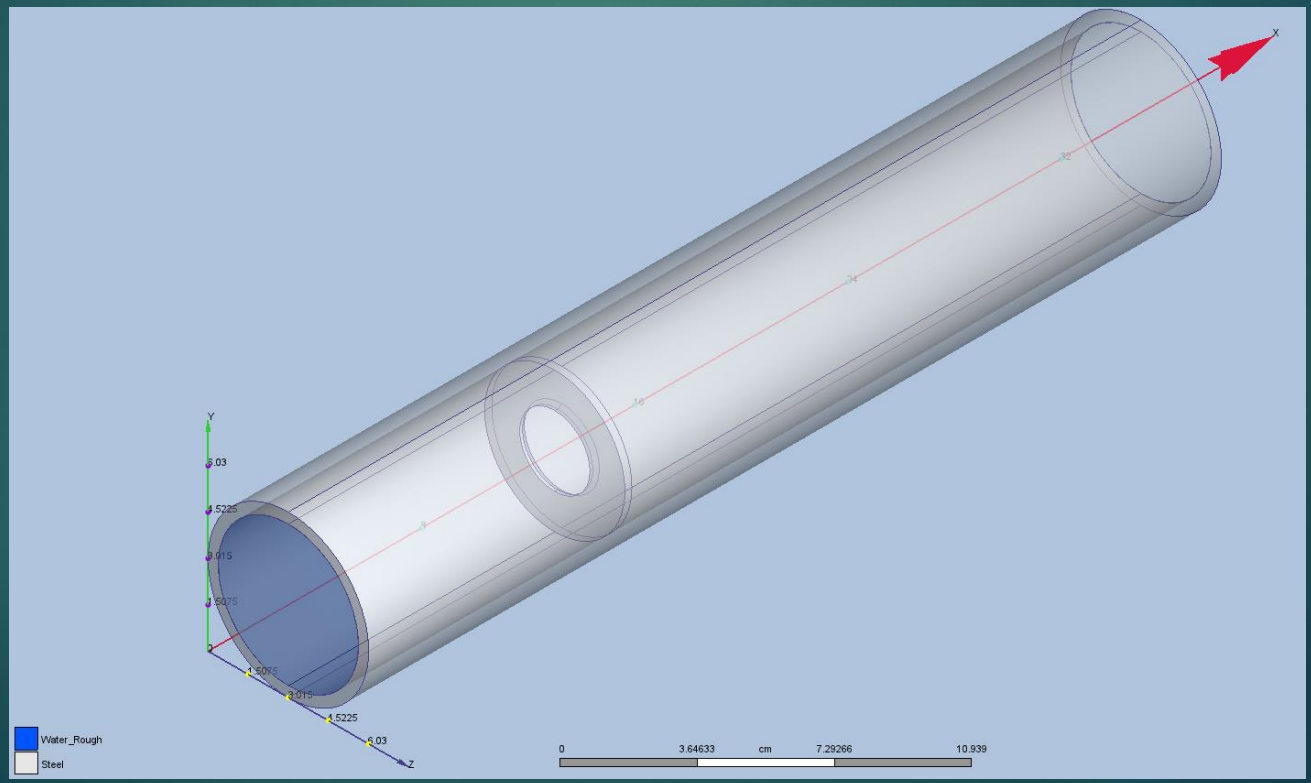

Mesh Definition

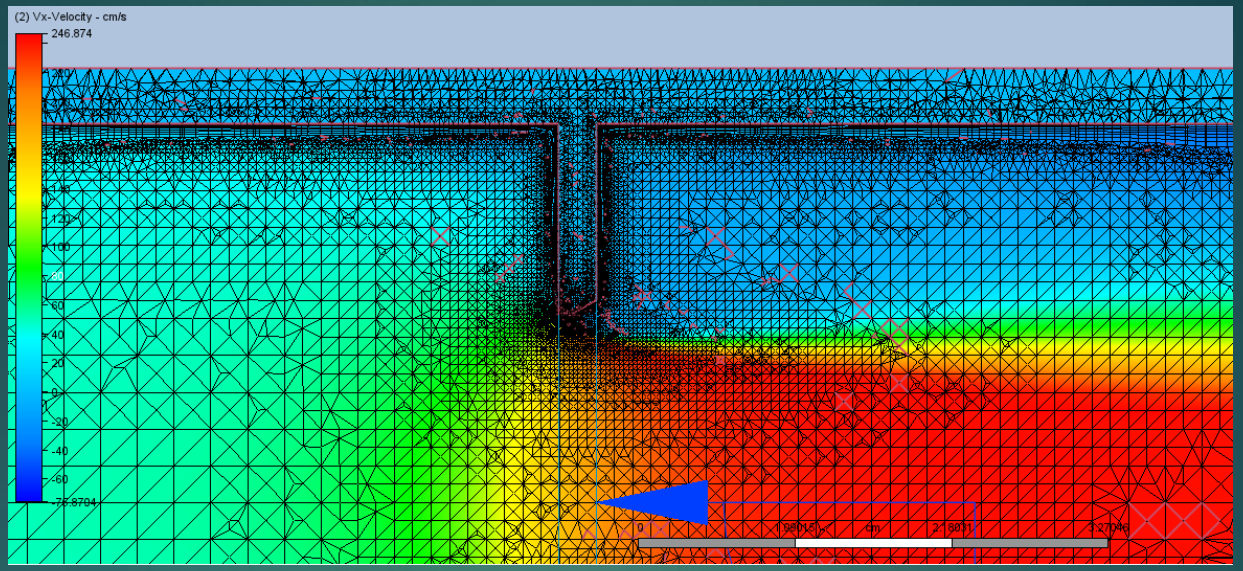

Refined mesh: 20.1 x 10^6 Fluid elements, 4.5 x 10^6 nodes

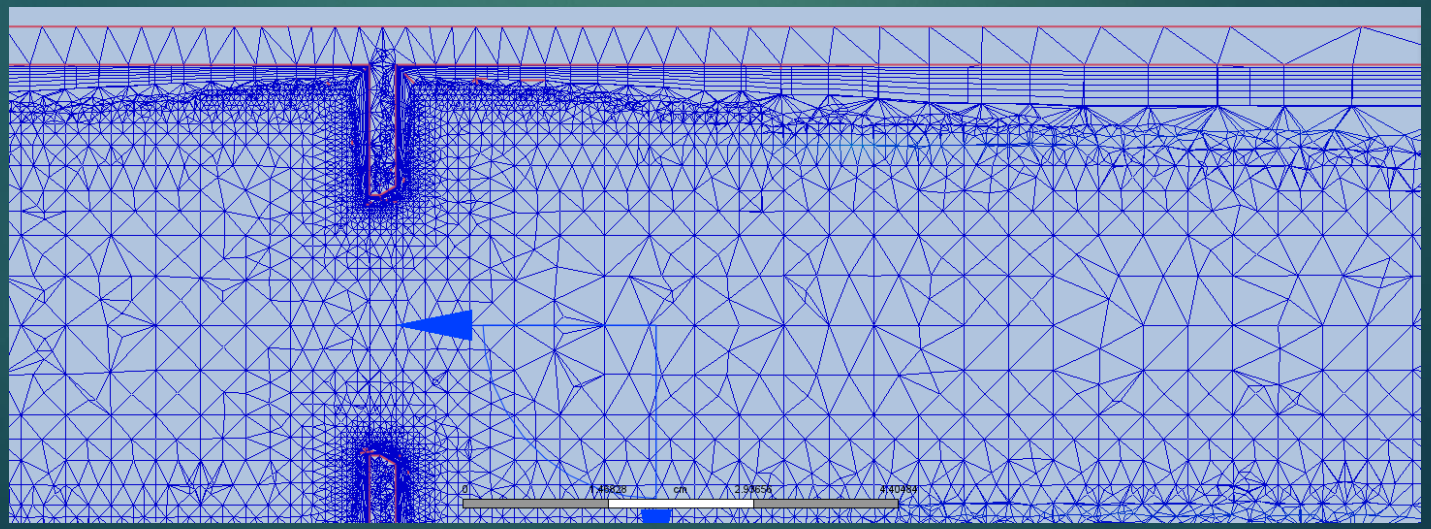

Reduced/Optimized mesh: ~1.4 x 10^6 elements (includes solid elements), 2.6 x 10^6 Nodes

CFD Simulation – k-Epsilon Turbulence Model

- Governing equations
  - Turbulent Kinetic Energy (TKE) Equation

$$\rho\frac{\partial K}{\partial t}+\rho U\frac{\partial K}{\partial x}+\rho V\frac{\partial K}{\partial y}+\rho W\frac{\partial K}{\partial z}$$
$$=\frac{\partial}{\partial x}\left[\left(\frac{\mu_t}{\sigma_K}\right)\frac{\partial K}{\partial x}\right]+\frac{\partial}{\partial y}\left[\left(\frac{\mu_t}{\sigma_K}\right)\frac{\partial K}{\partial y}\right]+\frac{\partial}{\partial z}\left[\left(\frac{\mu_t}{\sigma_K}\right)\frac{\partial K}{\partial z}\right]-\rho\varepsilon$$
$$+\mu_t\left[2\left(\frac{\partial U}{\partial x}\right)^2+2\left(\frac{\partial V}{\partial y}\right)^2+2\left(\frac{\partial W}{\partial z}\right)^2+\left(\frac{\partial U}{\partial y}+\frac{\partial V}{\partial x}\right)^2+\left(\frac{\partial U}{\partial z}+\frac{\partial W}{\partial x}\right)^2+\left(\frac{\partial V}{\partial z}+\frac{\partial W}{\partial y}\right)^2\right]$$

  - Turbulent Energy Dissipation (TED) Equation

$$\rho\frac{\partial \varepsilon}{\partial t}+\rho U\frac{\partial \varepsilon}{\partial x}+\rho V\frac{\partial \varepsilon}{\partial y}+\rho W\frac{\partial \varepsilon}{\partial z}$$
$$=\frac{\partial}{\partial x}\left[\left(\frac{\mu_t}{\sigma_\varepsilon}\right)\frac{\partial \varepsilon}{\partial x}\right]+\frac{\partial}{\partial y}\left[\left(\frac{\mu_t}{\sigma_\varepsilon}\right)\frac{\partial \varepsilon}{\partial y}\right]+\frac{\partial}{\partial z}\left[\left(\frac{\mu_t}{\sigma_{\varepsilon 2}}\right)\frac{\partial \varepsilon}{\partial z}\right]-C_2\rho\frac{\varepsilon^2}{K}$$
$$+C_1\mu_t\frac{\varepsilon}{K}\left[2\left(\frac{\partial U}{\partial x}\right)^2+2\left(\frac{\partial V}{\partial y}\right)^2+2\left(\frac{\partial W}{\partial z}\right)^2+\left(\frac{\partial U}{\partial y}+\frac{\partial V}{\partial x}\right)^2+\left(\frac{\partial U}{\partial z}+\frac{\partial W}{\partial x}\right)^2\right.$$

Constant	Value
C_μ	0.09
C_1	1.44
C_2	1.92
σ_K	1.0
σ_ε	1.3

These equations, combined with mass, momentum, and energy conservation equations, form a set of 9 equations with 9 unknowns $(U, V, W, P, T, \mu_t, k_t, K, \varepsilon)$ solved numerically

GE Discretization

- Finite element discretization scheme
  - Dependent variables are represented as polynomial shape function across fluid volume (element)
  - Shape functions substituted into governing PDEs then weighted integral taken over the element

$$\int_L \left[\frac{\partial \varphi}{\partial t} w_{t_i} + \left(a\frac{\partial \varphi}{\partial x} - D\frac{\partial^2 \varphi}{\partial x^2}\right) w_{s_i}\right] dx = 0$$

  - For Modified Petrov-Galerkin w_{t_i} and w_{s_i} are different
- Spatial Terms:
  - Finite element method directly applied to the diffusion and source terms where weight function = shape function
  - Upwind method and weighted integral method applied to advection terms – increases numerical stability
    - Upwind scheme: Modified Petrov-Galerkin used where "bubble functions" are added (upstream) and subtracted (downstream) to the shape functions
- Temporal terms:
  - Implicit/backward difference scheme ($\varphi = \mathrm{u, v, w} \ldots$)

$$\frac{\partial \varphi}{\partial t} \approx \frac{\varphi_{new} - \varphi_{old}}{\Delta t}$$

  - Each discretized transient equation must be solved iteratively at each time step to determine all of the new variable values

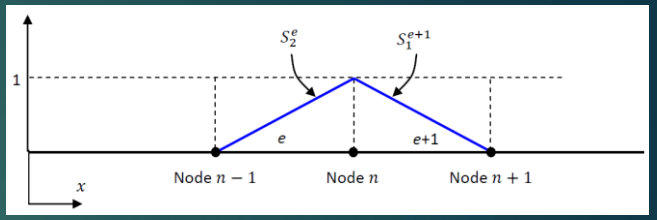

Examples of polynomial shape functions across fluid elements (1D case shown)

$$S_2^e = \frac{1}{2}(1+\xi)$$

$$S_1^{e+1} = \frac{1}{2}(1-\xi)$$

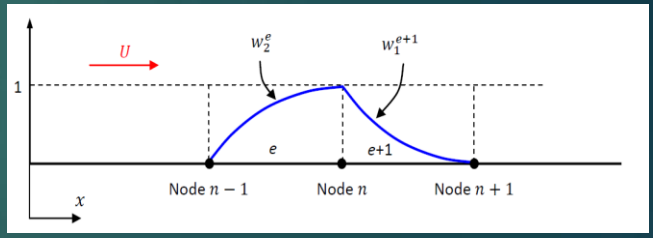

Upwinding applied to advection terms. Modifies weight function by adding a "bubble function"

$$w_2^e = \frac{1}{2}(1+\xi) + \frac{3}{4}\beta(1-\xi^2)$$

$$w_1^{e+1} = \frac{1}{2}(1-\xi) - \frac{3}{4}\beta(1-\xi^2)$$

CFD Simulation – k-Epsilon Axial Velocity Results

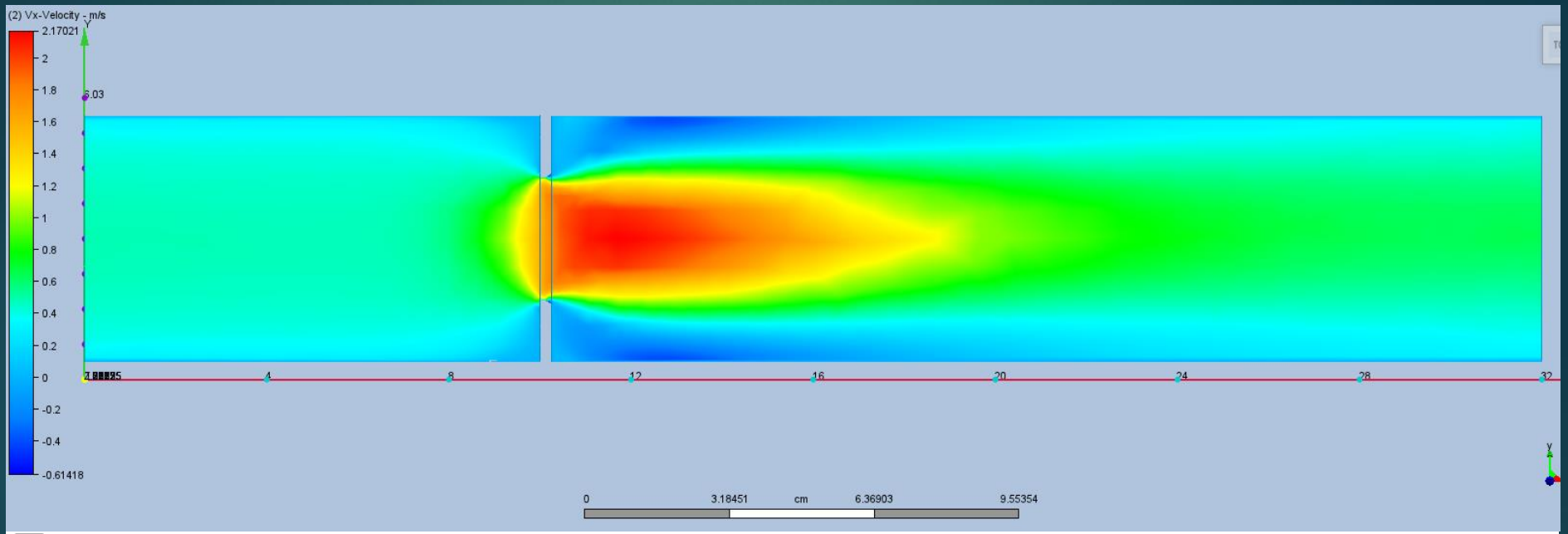

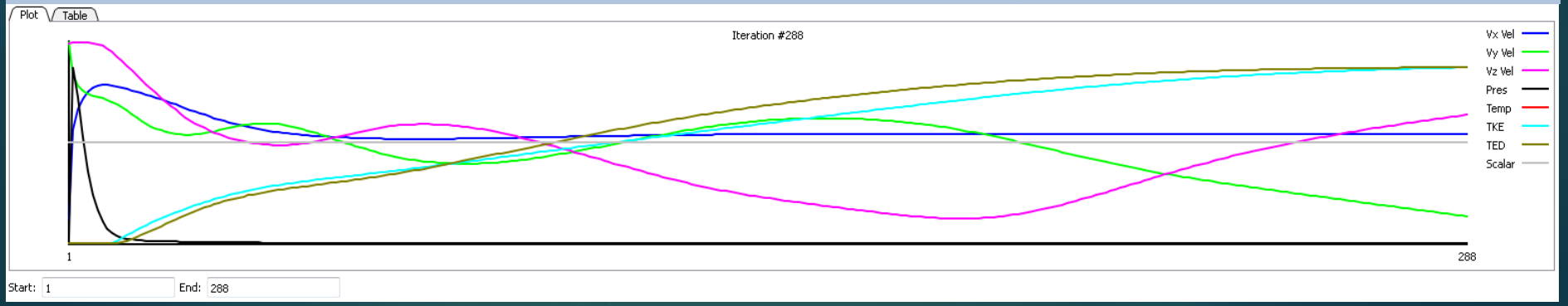

K-Epsilon Algorithm Results

- Numerically stable but inaccurate solution
  - Discontinuity at the wall persisted for all mesh refinement levels – law of the wall seems to be inaccurately implemented within CFD software
  - Peaked central flow profile

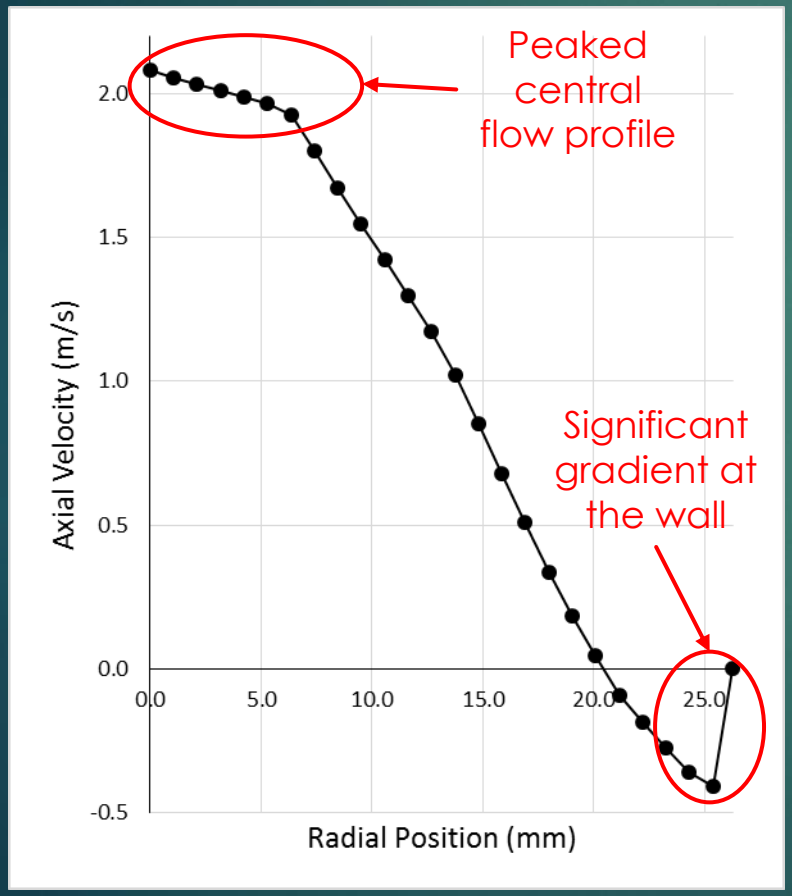

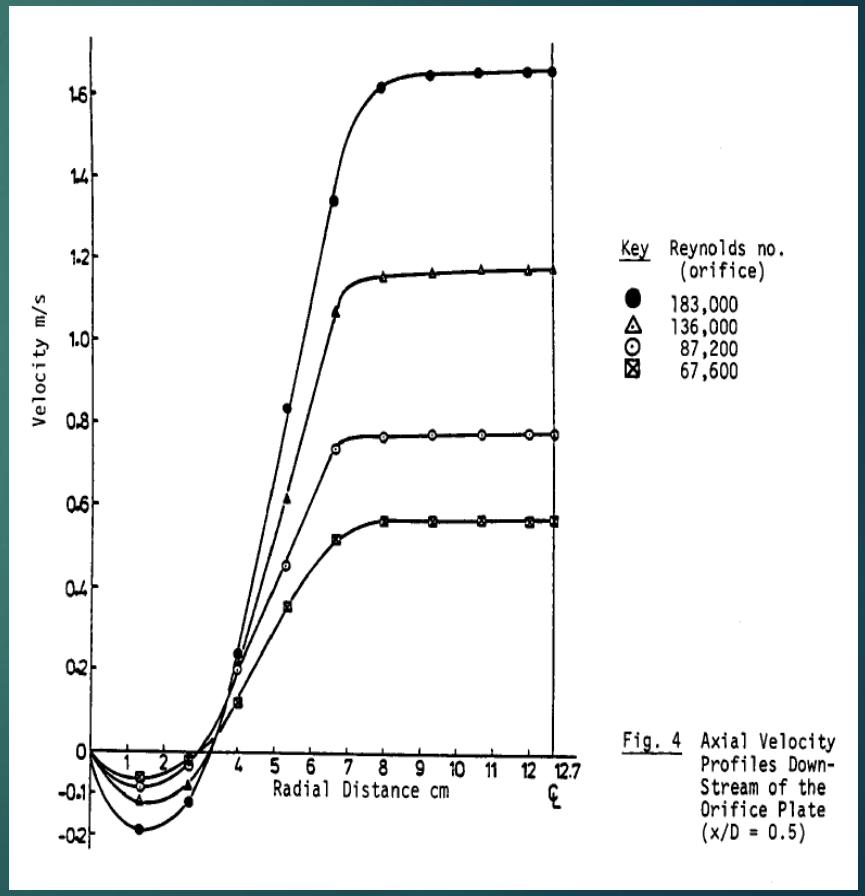

CFD Simulation – SST k-Omega Turbulence Model

- Hybrid model combining the Wilcox k-omega and the k-epsilon models.
  - Wilcox k-omega model used near the wall, k-epsilon used in free stream
- Governing equations
  - Modification to Turbulent Kinetic Energy (TKE) Equation

$$\frac{\partial k}{\partial t} + U_j \frac{\partial k}{\partial x_j} = P_k - \beta^* k\omega + \frac{\partial}{\partial x_j}\left[(\nu + \sigma_k \nu_T)\frac{\partial k}{\partial x_j}\right]$$

  - Convert TED equation to Specific Dissipation Rate (ω)equation

$$\frac{\partial \omega}{\partial t} + U_j \frac{\partial \omega}{\partial x_j} = \alpha S^2 - \beta \omega^2 + \frac{\partial}{\partial x_j}\left[(\nu + \sigma_\omega \nu_T)\frac{\partial \omega}{\partial x_j}\right] + 2(1 - F_1)\frac{1}{\omega}\frac{\partial k}{\partial x_i}\frac{\partial \omega}{\partial x_i}$$

  - F_1 is a blending function that activates Wilcox model near the wall and the k-epsilon model in the free stream.

Variable	Definition
P_k	$\min\left(\tau_{ij}\frac{\partial U_i}{\partial x_j}, 10\beta^* k\omega\right)$
ν_T	$\frac{a_1 k}{\max(a_1\omega, SF_2)}$
F_1	$tanh\left\{\left\{min\left[max\left(\frac{\sqrt{k}}{\beta^*\omega y}, \frac{500\nu}{y^2\omega}\right), \frac{4\sigma_{\omega 2}k}{CD_{k\omega}y^2}\right]\right\}^4\right\}$
F_2	$tanh\left[\left[max\left(\frac{\sqrt{k}}{\beta^*\omega y}, \frac{500\nu}{y^2\omega}\right)\right]^2\right]$
$CD_{k\omega}$	$\max\left(2\rho\sigma_{\omega 2}\frac{1}{\omega}\frac{\partial k}{\partial x_i}\frac{\partial \omega}{\partial x_i}, 10^{-10}\right)$

Constant	Value
$\beta^*, \beta_1, \beta_2$	$\frac{9}{100}, \frac{3}{40}, 0.0828$
α_1, α_2	$\frac{5}{9}, 0.44$
σ_{k1}, σ_{k2}	$0.85, 1$
$\sigma_{\omega 1}, \sigma_{\omega 2}$	$0.5, 0.856$

These equations, combined with mass, momentum, and energy conservation equations, form a set of 9 equations with 9 unknowns ($U, V, W, P, T, \mu_t, k_t, k, \omega$) solved numerically

SST k-Omega – Axial Velocity Results

- Convergence: 255 iterations
- Inlet mean velocity= 0.4 m/s (fully developed flow profile)
- Maximum Velocity = 2.5 m/s
- Reynolds Number =~67,000

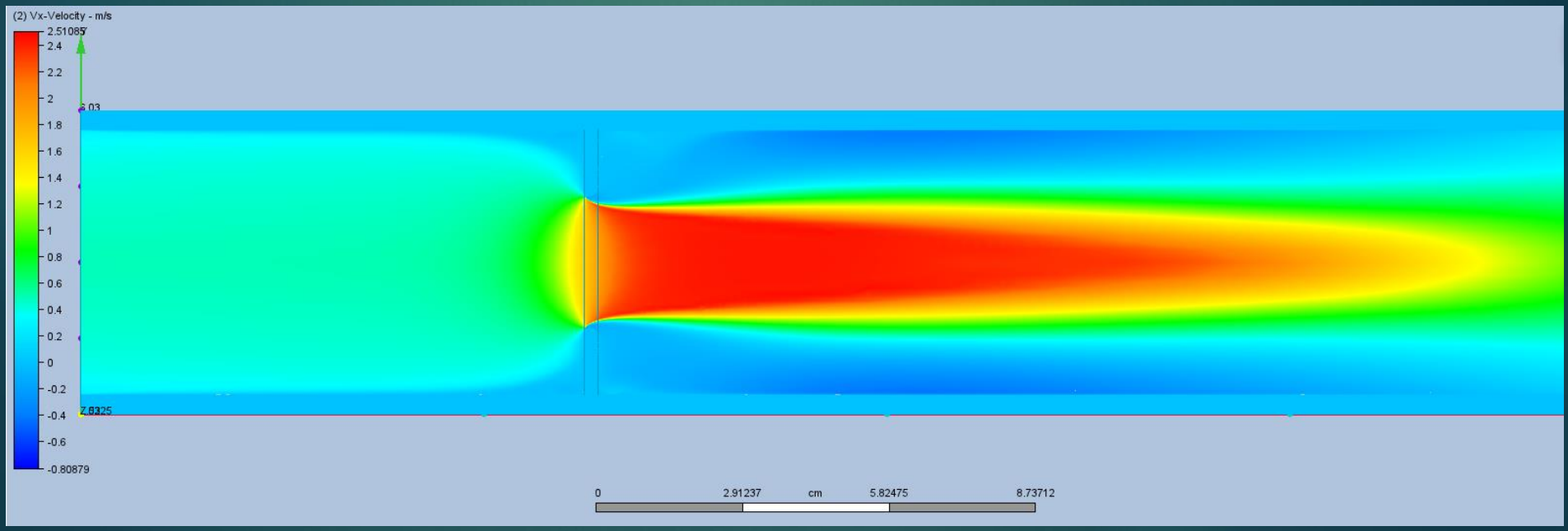

CFD Simulation – SST k-Omega Results

- Resolved issues with peaked central flow
- Gradient at the wall reduced
- Some what consistent across both mesh sizes
  - Adequate solution considering that which ever solution is chosen will be the reference for comparison when evaluating PET reconstructed flow fields.

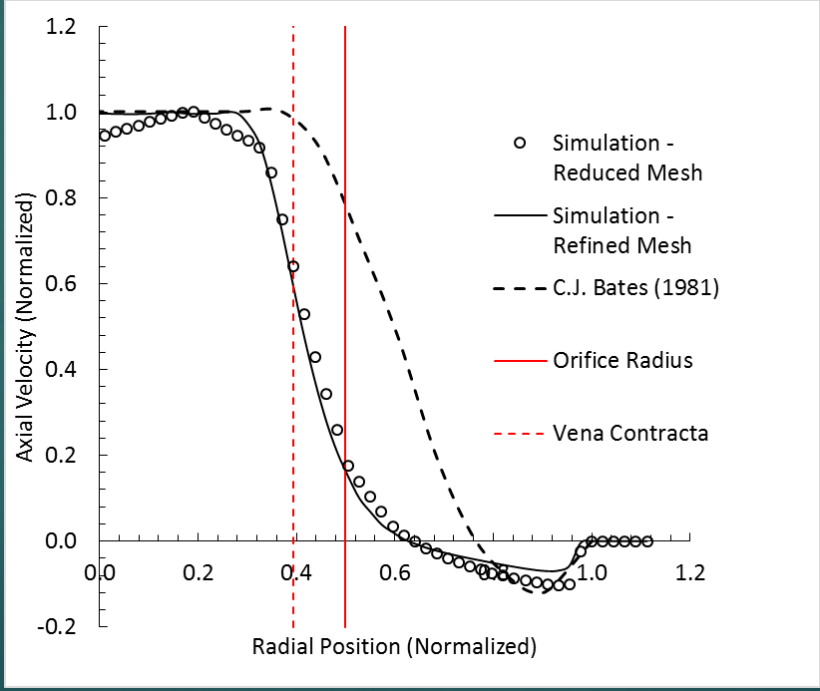

Axial velocity profiles at x/D = 0.5

SST k-Omega Results

- Axial velocity results at x/D=1.0 are comparable in the central flow region and to CFD results from Ahmed (2012)
  - $k-\varepsilon$ (RNG) differential viscosity turbulence model used to account for low-Reynolds-number (LRN) effects
  - Recirculating region and Near wall solutions for current study are in closer agreement than RNG-based CFD results.
- Approximate comparison of measured data (Bates-1981) at x/d = 0.9 - consistent shift from measured data .

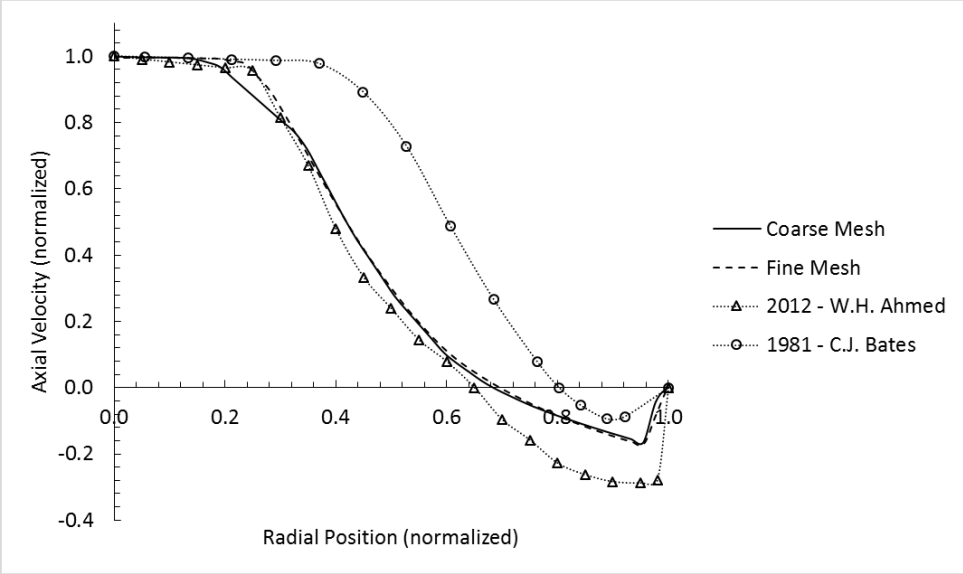

Axial velocity profiles at x/D = 1.0 (Bates (1981) x/D = 0.9)

SST k-Omega – TKE Results

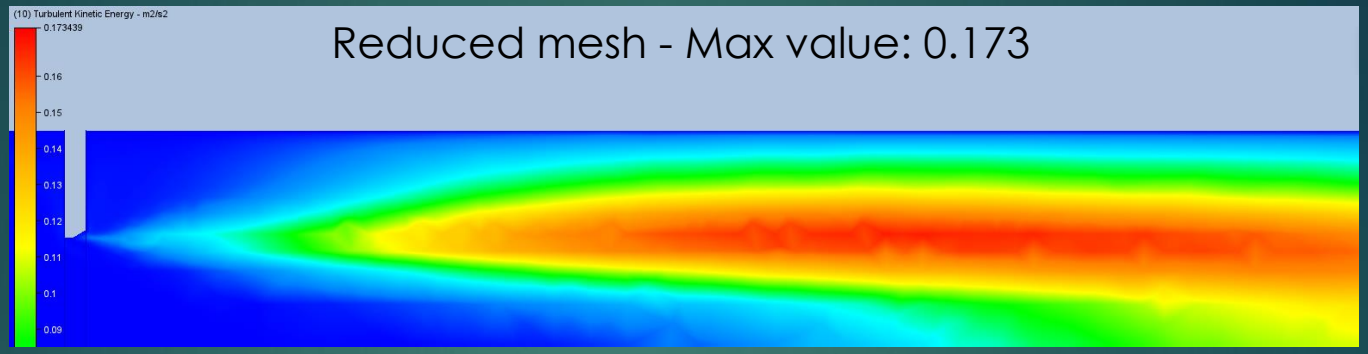

Reduced mesh - Max value: 0.173

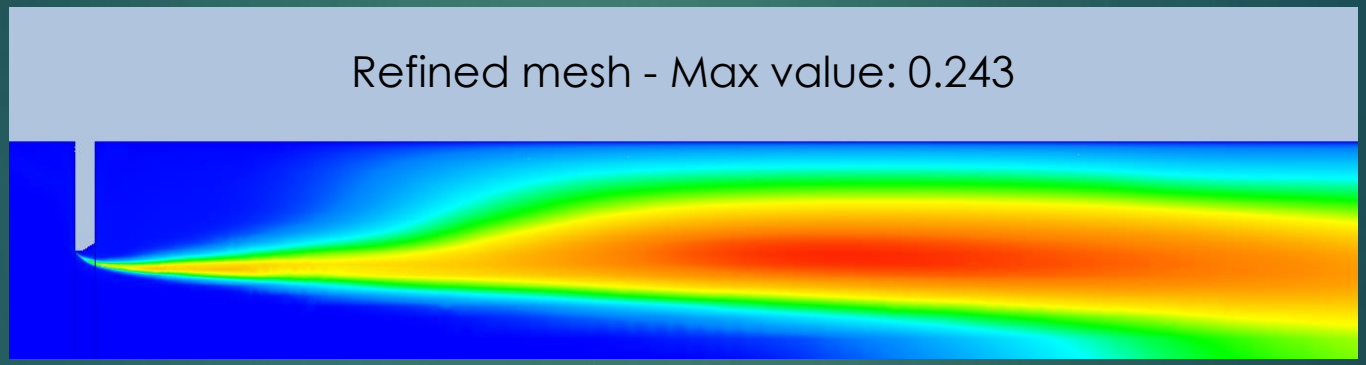

Refined mesh - Max value: 0.243

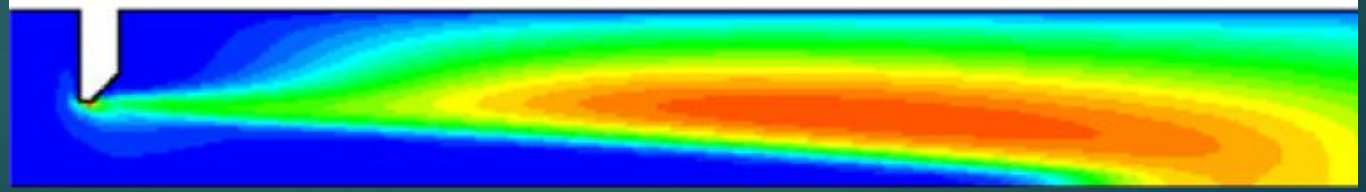

W.H. Ahmed (2012) - Max value: 0.243

SST k-Omega – TKE Results

- Turbulent kinetic energy profiles normalized to the square of the mean inlet velocity (nondimensionalized)
  - Provides an indication of the turbulence intensity which drives advective diffusion rates of radioisotopes into the recirculating region of the flow.
- Reduced Mesh shows higher TKE compared to measured data – Results in conservatively high radioisitope diffusion rate
- Proceed with transient scalar transport simulation with reduced mesh steady state results.

Non-dimensionalized Turbulent Kinetic Energy Radial Profiles

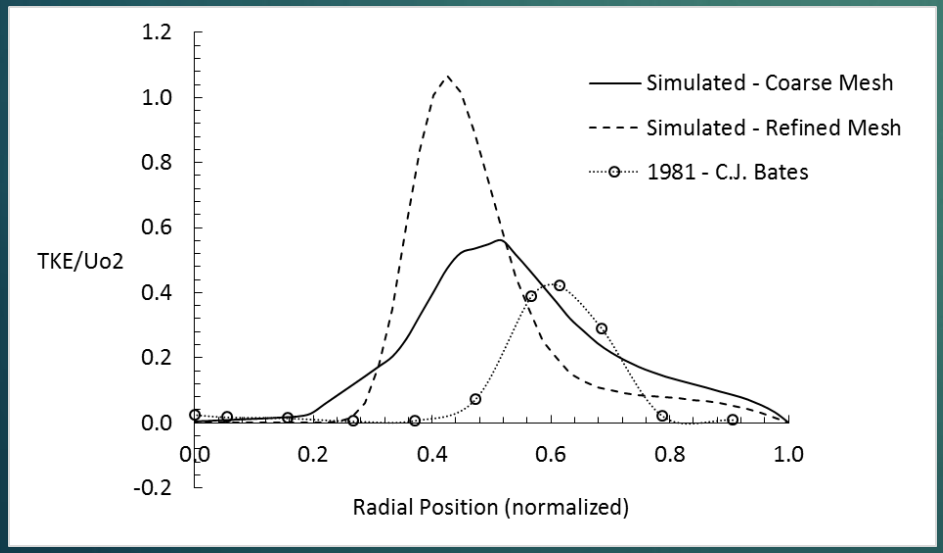

x/D = 0.5

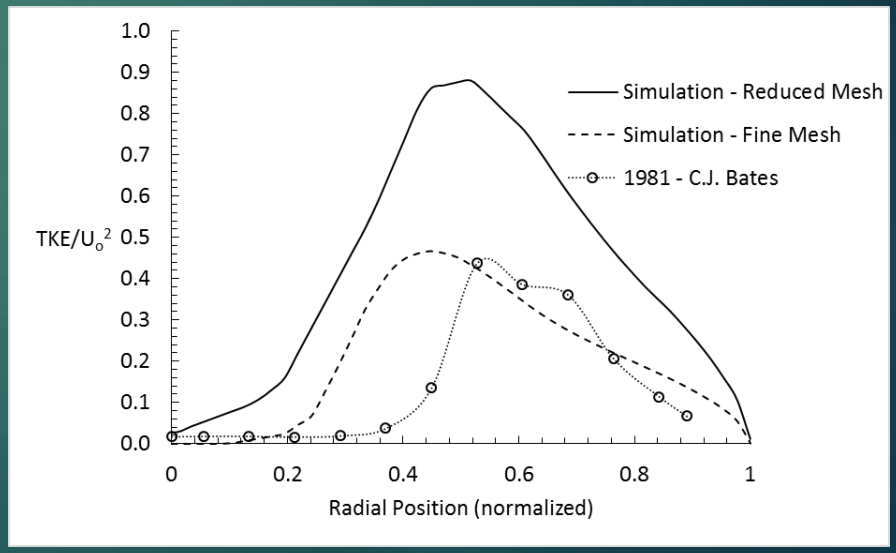

x/D = 1.0 (Bates (1981) x/D = 0.9)

Computational Fluid Dynamics – Transient Scalar Transport Simulation

SECTION 3

Governing Equations

- Governing Equations for passive scalar transport through an incompressible fluid.[Ref. 4]

$$\frac{\partial f}{\partial t}+u\frac{\partial f}{\partial x}+v\frac{\partial f}{\partial y}+w\frac{\partial f}{\partial z}=\frac{\partial}{\partial x}\left[D\frac{\partial f}{\partial x}\right]+\frac{\partial}{\partial y}\left[D\frac{\partial f}{\partial y}\right]+\frac{\partial}{\partial z}\left[D\frac{\partial f}{\partial z}\right]$$

- For turbulent flow - time averaged and assuming the scalar value can be represented by $f = F + f'$ results in

$$\frac{\partial F}{\partial t}+u\frac{\partial F}{\partial x}+v\frac{\partial F}{\partial y}+w\frac{\partial F}{\partial z}=\frac{\partial}{\partial x}\left[D\frac{\partial F}{\partial x}-uf\right]+\frac{\partial}{\partial y}\left[D\frac{\partial F}{\partial y}-vf\right]+\frac{\partial}{\partial z}\left[D\frac{\partial F}{\partial z}-wf\right]$$

- Boussinesq Approximation and isotropic turbulence assumption used to relate the new terms generated from the averaging process to the mean values (F) using eddy diffusivity.

$$D_t=\frac{-uf}{\frac{\partial F}{\partial x}}=\frac{-vf}{\frac{\partial F}{\partial y}}=\frac{-wf}{\frac{\partial F}{\partial z}}$$

- Applying to the averaged scalar equation

$$\frac{\partial F}{\partial t}+u\frac{\partial F}{\partial x}+v\frac{\partial F}{\partial y}+w\frac{\partial F}{\partial z}=\frac{\partial}{\partial x}\left[D_t\frac{\partial F}{\partial x}\right]+\frac{\partial}{\partial y}\left[D_t\frac{\partial F}{\partial y}\right]+\frac{\partial}{\partial z}\left[D_t\frac{\partial F}{\partial z}\right]$$

- Leaves only the eddy diffusivity to be calculated using the eddy viscosity and turbulent Schmidt number ($\sigma_t = 1$ usually)

$$D_t=\frac{\mu_t}{\sigma_t}$$

Simulation parameter

- Boundary conditions:
  - Inlet Scalar Value: Ramp step with normalized max value: Normalized to $0.36\ {}^{MBq}/_{cm^3}$
- Initial condition: radioisotope (scalar) concentration at each surface = 0
- Time step: 0.001 seconds
  - CFL=~40 based on smallest element size and velocity at the element → implicit scheme less susceptible to numerical instability with CFL >1.
- Inner iterations (iterations per time step): 3
- Mesh: Reduced

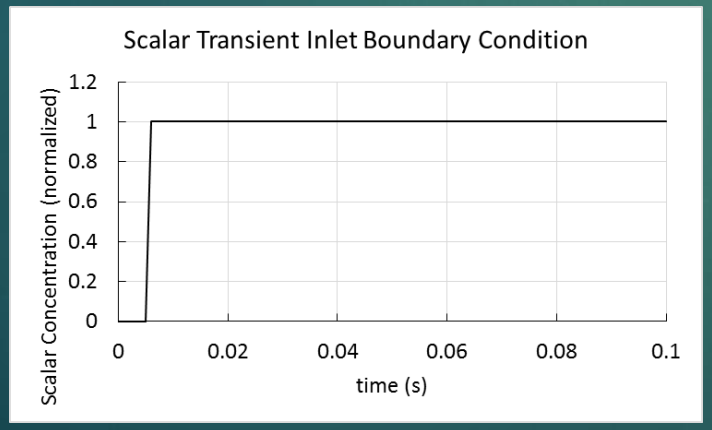

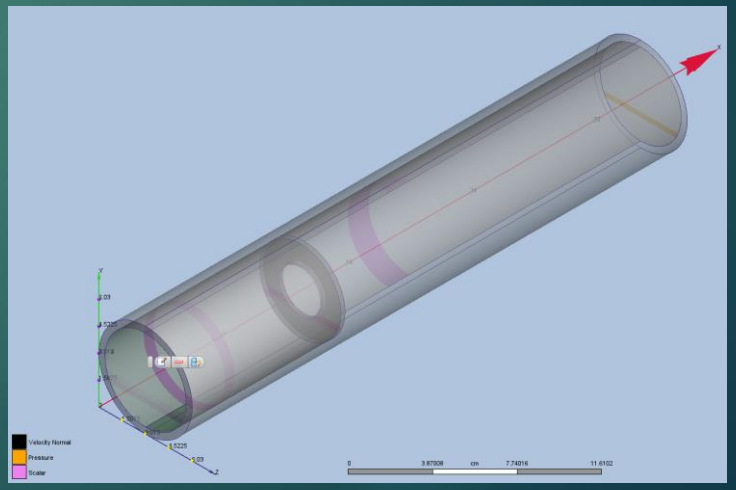

Radioisotope Transport Results

- Simulation ran to 7 seconds
  - Asymptotically approaches uniform distribution with visible indicators of upstream and downstream recirculation regions

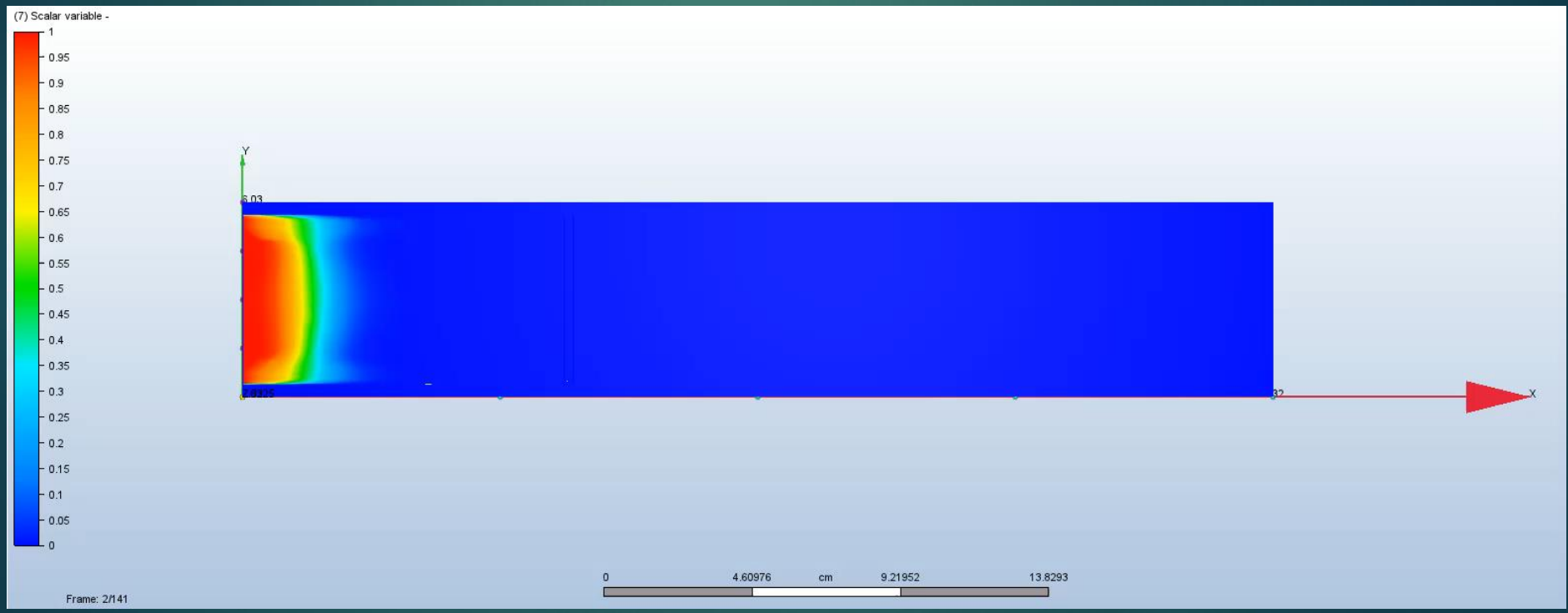

CFD Forward work

- Generate a script that converts the CFD software's output file format into a GATE input file (macro) format for each time step.
- Run longer scalar transport simulation
- Run additional Re cases.

GEANT4 Applications for Tomographic Emission (GATE)

SECTION 6

GATE Simulation Architecture

- GATE software is a wrap around software that utilizes Monte Carlo simulation-based GEANT4 Physics package
- Simulates most aspects of a PET system that influences detector response to beta+ decay and annihilation process within the system's field of view (FOV)

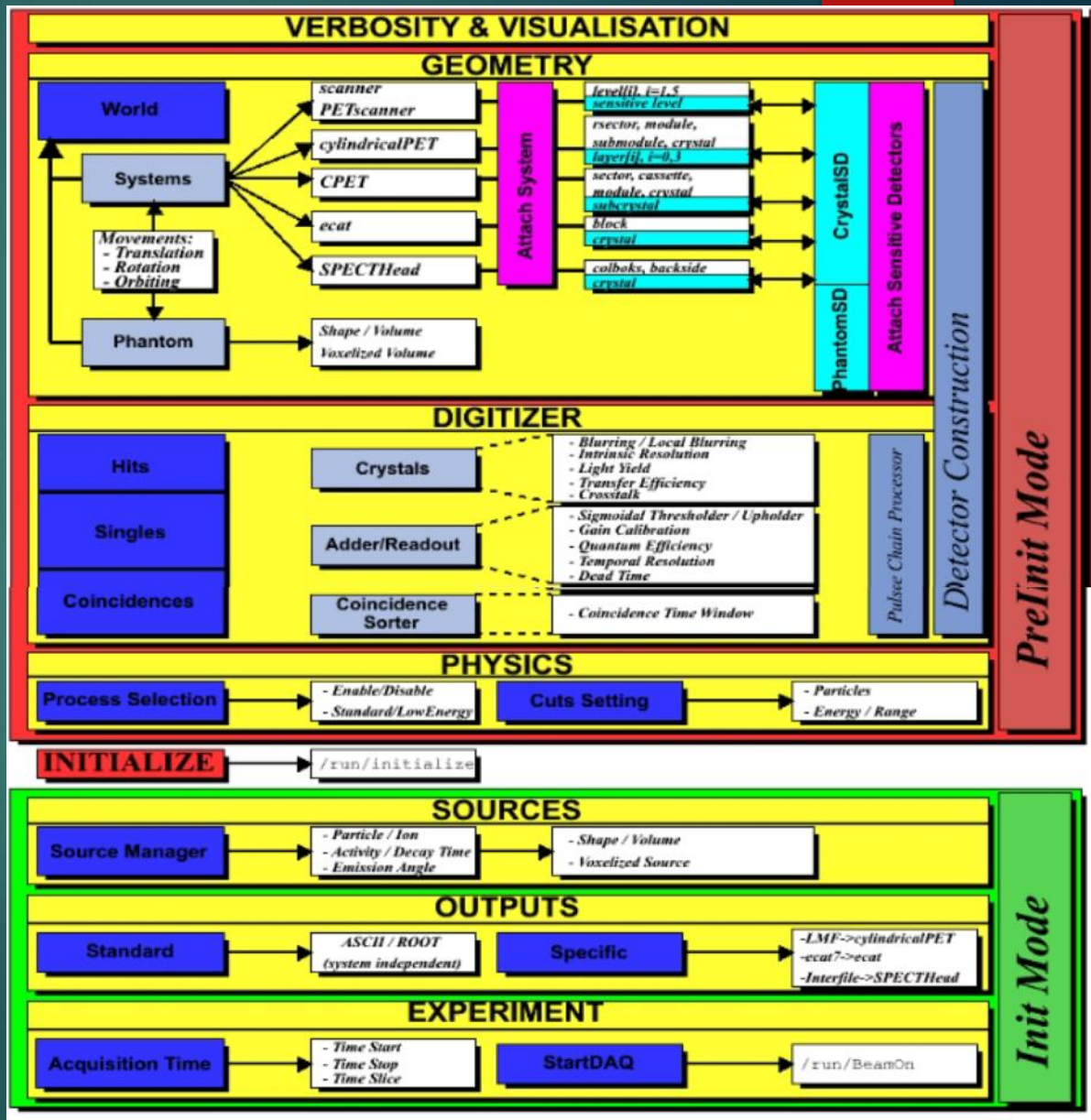

PET System Description

- Seimens Inveon PET/CT system
  - Tungsten end shields
  - Scintillating crystals: lutetium oxyorthosilicate (LSO)
  - 16 radial sectors with 4 axial x 1 radial array of modules(blocks)
  - Each block: 20 x 20 LSO crystal array each crystal element is 1.59 mm x 1.59 mm x 10 mm
  - Total of 25,600 detector crystals
  - Ring inner diameter: 16.1 cm
  - Axial FOV: 12.7 cm
  - Transverse FOV: 10.0 cm.
  - Electronics: 64 acquisition channels, each detector is coupled via a light guide to a position-sensitive photomultiplier tube (PSPMT).
  - Output of each PSPMT is fed to and processed by a preamplifier electronics stack.

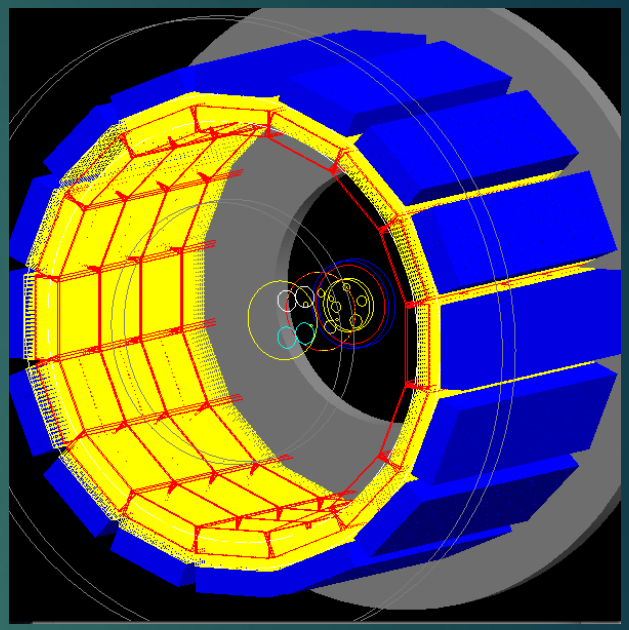

3D visualization of Seimens inveon PET system with NEMA NU4 Phantom in FOV – Visualization through OpenGL

Digitizer Definition

- Energy Window: 350 keV to 650 keV
- Coincidence timing window: 3.432 nsec
- Energy resolution (simulated Gaussian blurring): 0.146 keV centered at 511keV
- Deadtime: 7 msec; mode: Paralysable

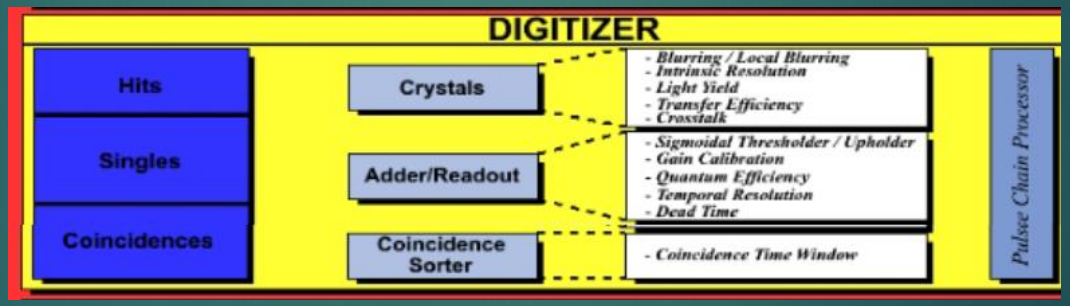

Physics Definition

- GEANT4 modules enabled:
  - F-18 Radioactive decay –
    - Positron (β^+) decay process of F-18 and transport of β^+ through surrounding media
  - Positron Annihilation – annihilation with electrons (β^-) and subsequent emission of two 511 keV gamma rays in opposite directions
  - Compton Scattering – Gamma photon primary interaction with matter at 511keV range.
    - Incident gamma photon loses enough energy to an atomic electron to cause its ejection
    - Remainder of the original photon's energy emitted as a new, lower energy gamma photon with emission direction different from incident direction.
  - Photoelectric - gamma photon interacts with and transfers its energy to an atomic electron, causing the ejection of that electron from the atom.
  - Rayleigh Scattering – elastic scattering of gamma photons
  - Electron Ionization – material ionization caused by gamma radiation
  - Bremsstrahlung Radiation - electromagnetic radiation produced by the deceleration of a charged particle when deflected by another charged particle.
  - Multiple Scattering: β^+ and β^- - transport of β^+ through surrounding media

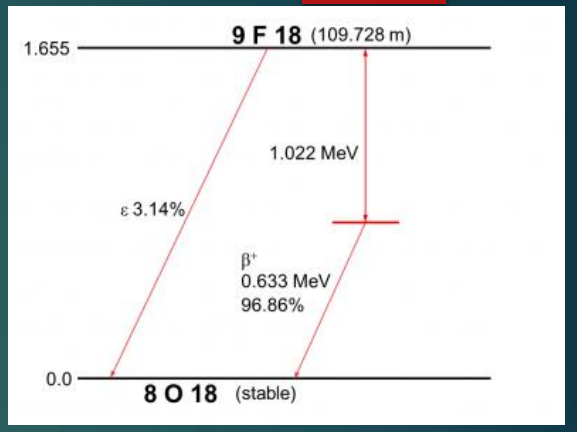

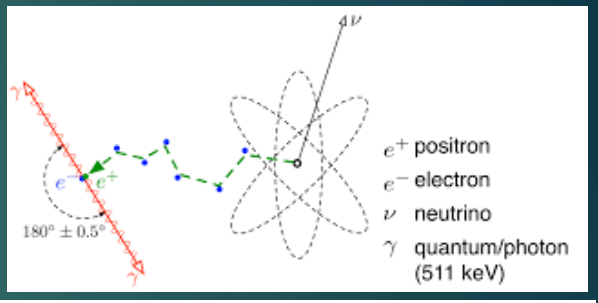

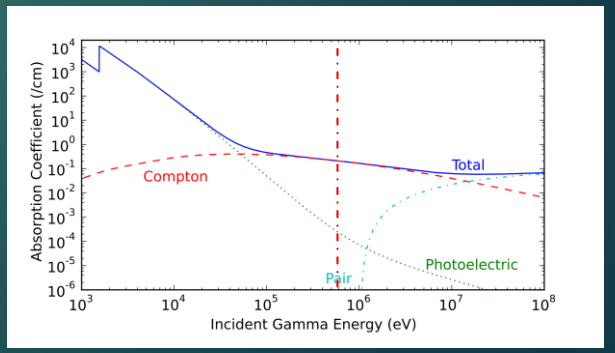

Absorption coefficient of Al (atomic number 13) showing typical contributions of the 3 effects.

Phantom/Source Definition

- Validation sources tested
  - NEMA 4U Image Quality:
    - Overall external dimensions: 33.5 mm dia. x 66 mm height

high-density polyethylene (blue)

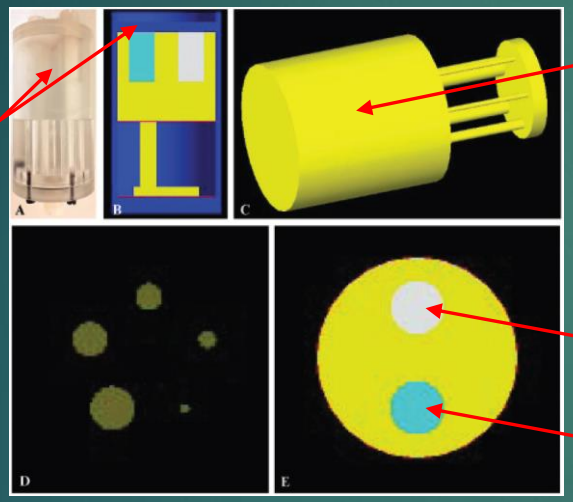

F-18/Water solution (activated) (yellow)

NEMA NU-4 Image Quality phantom picture

Unactivated Air (white)

Unactivated Water (cyan)

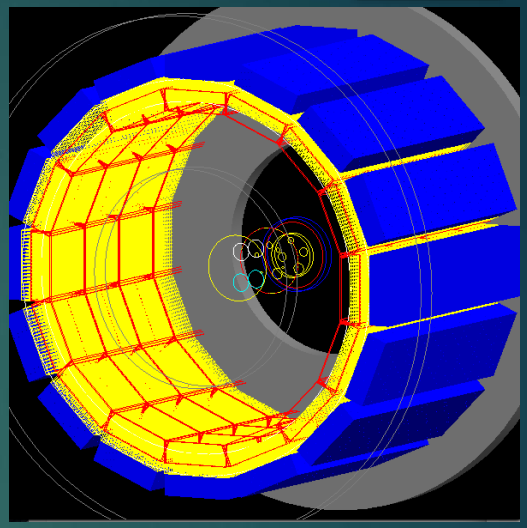

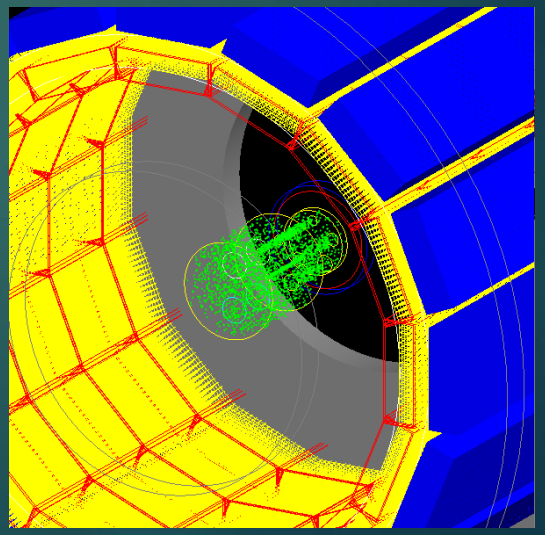

  - Cylinder: F-18/Air mixture; Dia.= 30 mm x Length=30 mm
  - Sphere: F-18/Air mixture; Dia. = 20mm
  - All sources assigned specific activities of $\sim 3.0\ \frac{kBq}{cm^3}$

GATE Validation Effort

- Several simulations of the NEMA NU4 IQ phantom have been ran in order to compare with published results (actual and simulated)

Run ID	Phantom/ Source	Total Acquisition Time (sec)	Time Slice Duration (sec)	Computer Run Time (sec)	
Run01*	NEMA NU-4 IQ	30	30	2100	
Run 01a†	NEMA NU-4 IQ	30	30	600	← Parallel processing implemented
Run 05a	NEMA NU-4 IQ	600	600	196 (min.)	← Used for comparison to reference simulation
Run 06	NEMA NU-4 IQ	0.5	0.1	10	
Run 07a	NEMA NU-4 IQ	0.5	.001	15	← Representative of CFD time step
Test_01a	Cylinder	30	30	~600	⎫
Test_02	Cylinder	5	5	~100	⎬ Troubleshooting STIR
Test_05	Sphere	10	10	~200	⎭

GATE Validation – Time Histograms

- ROOT software used to generate coincident detection histograms & projections
- Time histograms show relatively constant detection levels over short duration acquisitions
- Decay in count ray corresponding to exponential decay exhibited in 10 min acquisition (Run 05a)

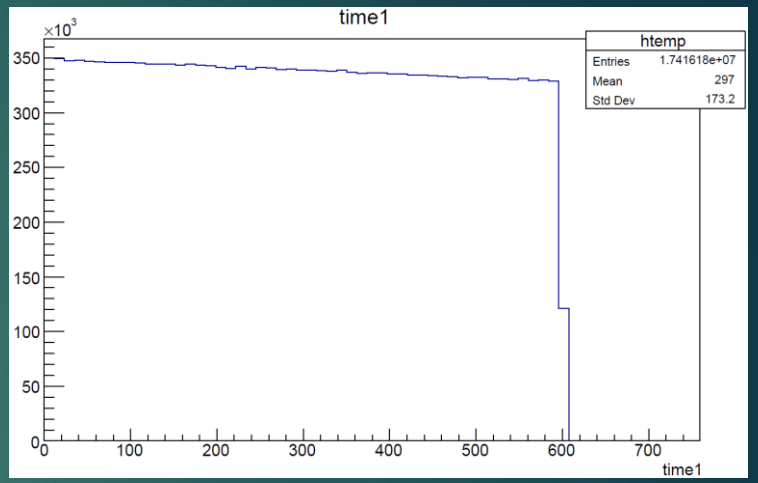

Run 05a Detections as a function of time

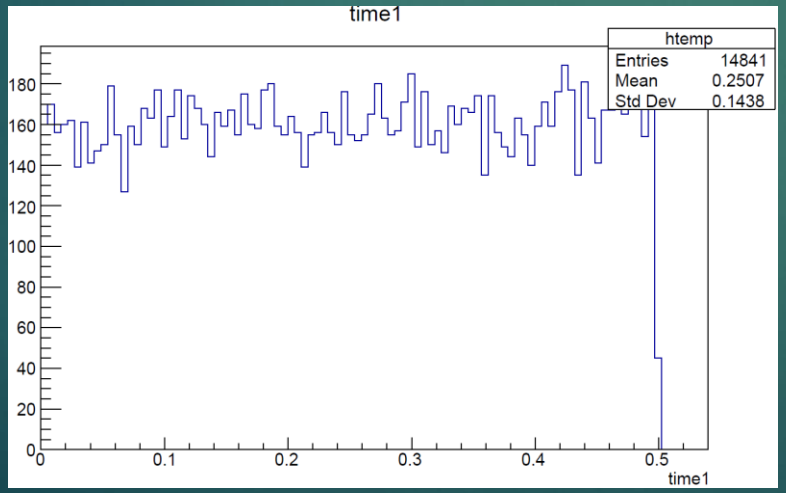

Run 06 Detection as a function of time

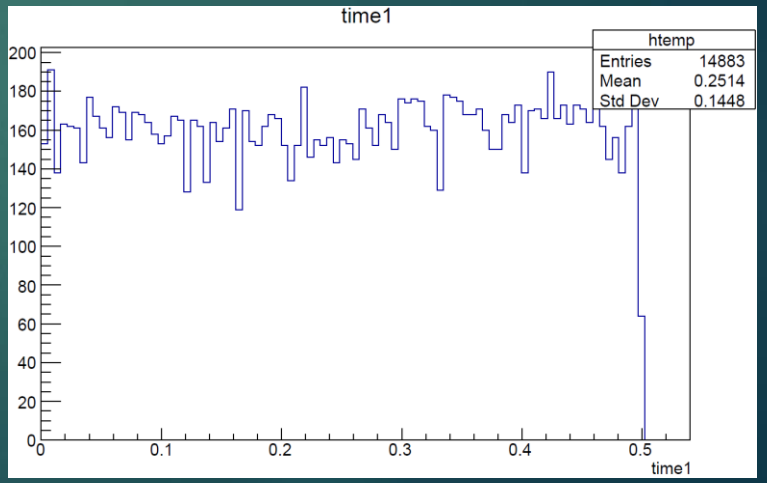

Run 07a Detection as a function of time

GATE Validation – Energy Spectra

- Energy spectrum showing good agreement with published LSO energy spectrum for 511 keV gamma photon

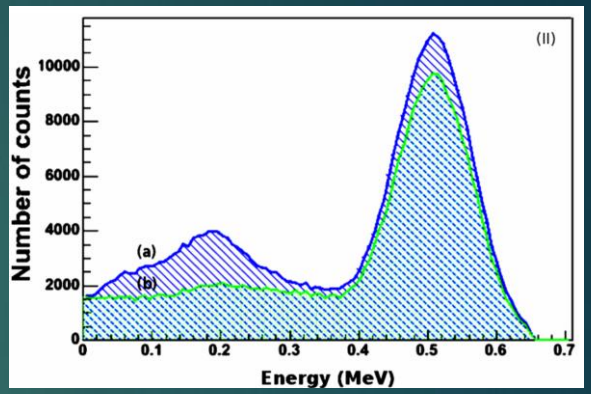

Reference F-18 Energy Spectrum as measured using LSO based PET Detector (2013 – D. Nikolopoulos *et. al.)*

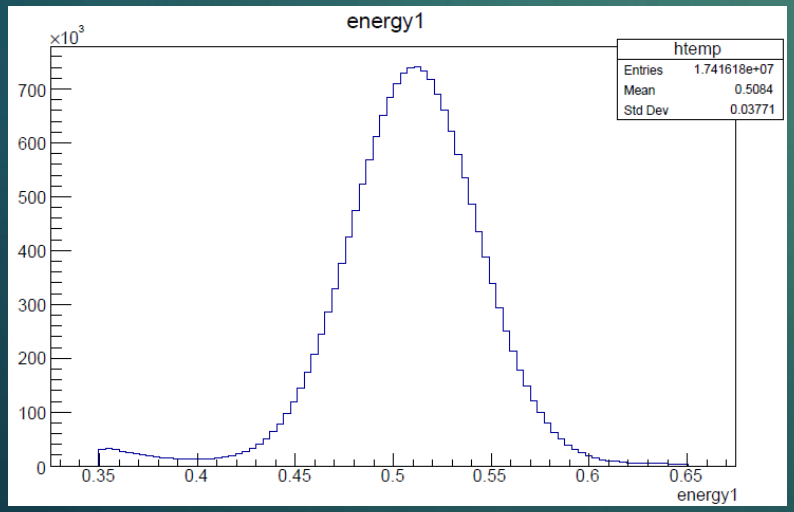

Run 05a Energy Spectrum

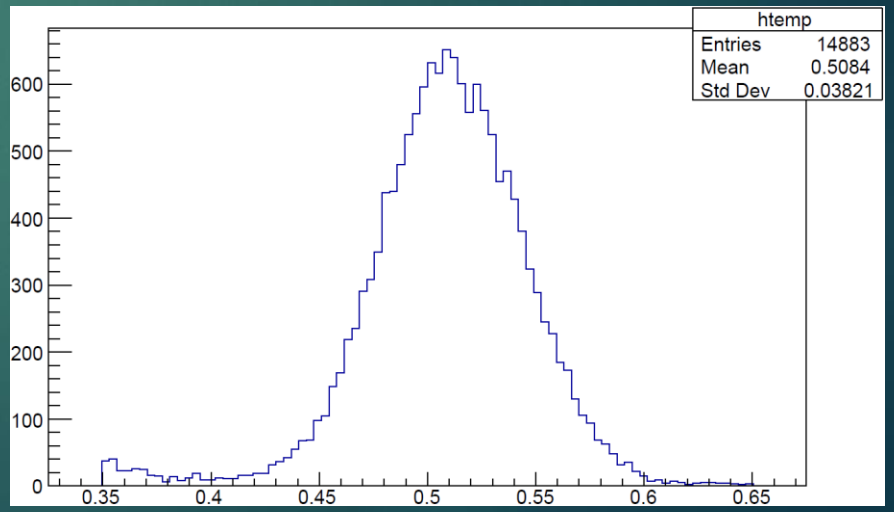

Run 07a Energy Spectrum

GATE Validation – Source Projections

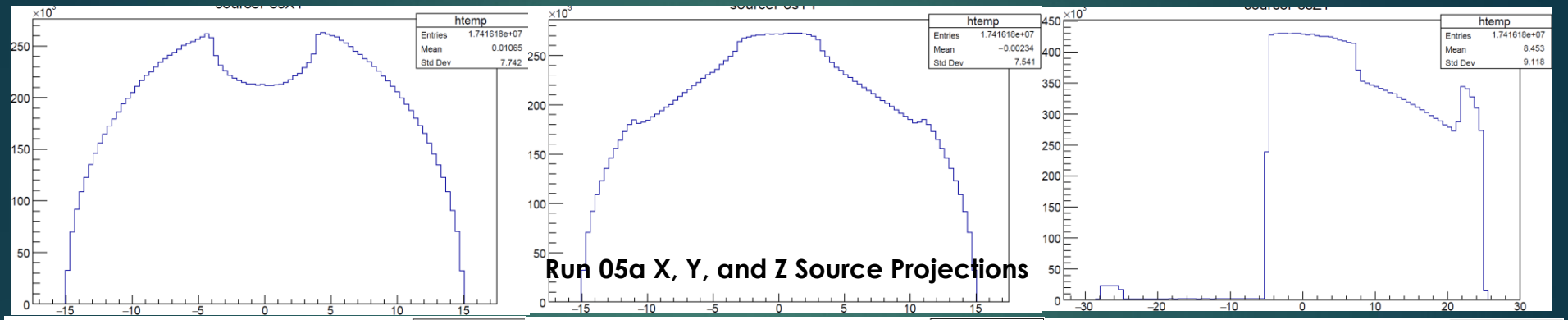

Run 05a X, Y, and Z Source Projections

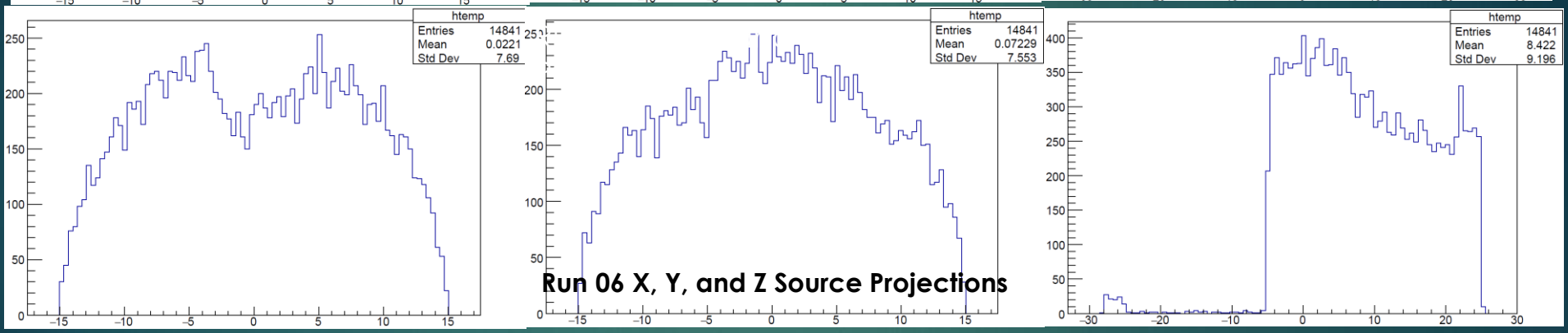

Run 06 X, Y, and Z Source Projections

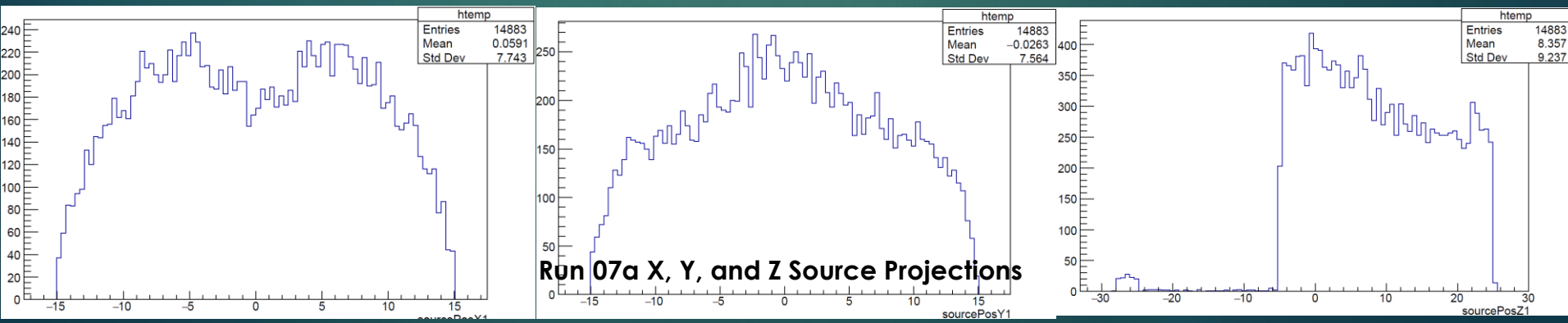

Run 07a X, Y, and Z Source Projections

GATE Validation – Source Projections

- Projections of cylindrical and spherical test sources are as expected
  - Test 01 Note: tapering of z projection due to variability of detector system sensitivity throughout FOV is observable

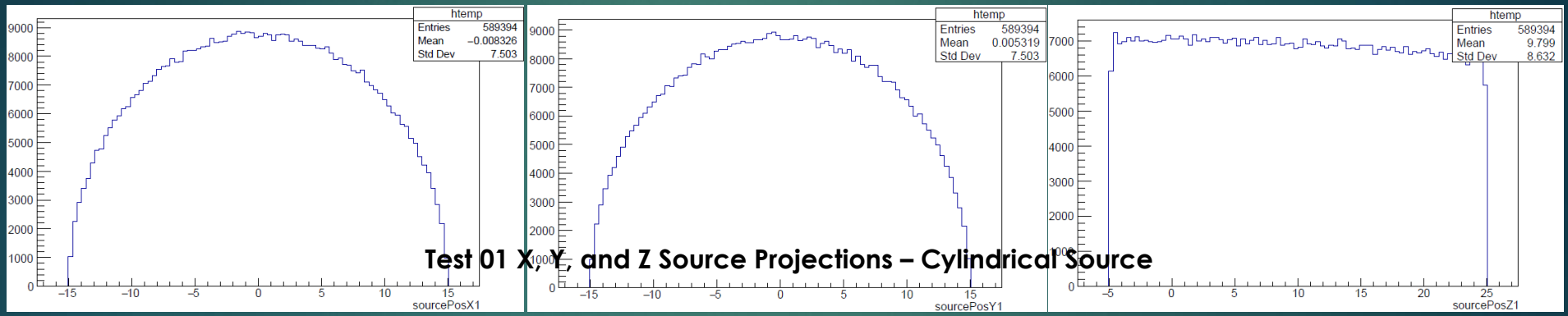

Test 01 X, Y, and Z Source Projections – Cylindrical Source

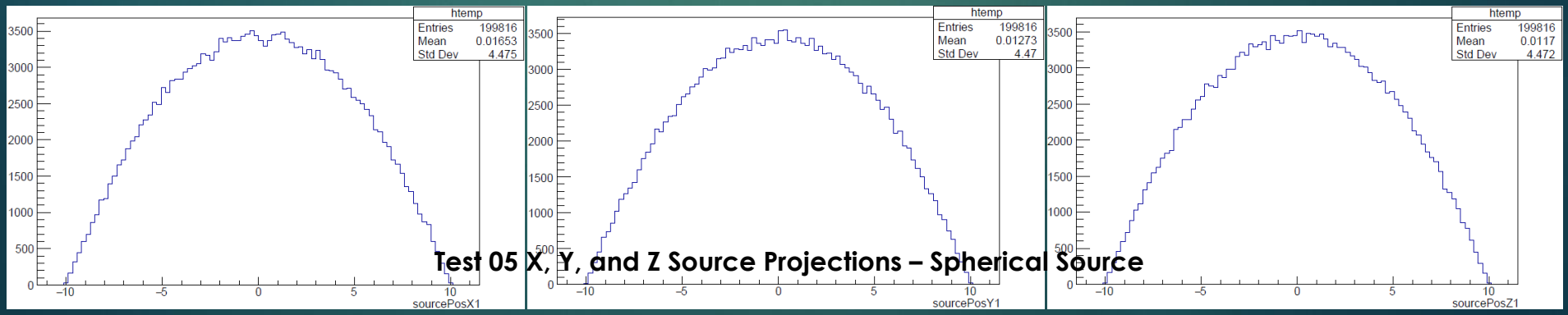

Test 05 X, Y, and Z Source Projections – Spherical Source

Image Reconstruction – Software for Tomographic Image Reconstruction (STIR)

SECTION 6

Image Reconstruction Algorithm

- Image Reconstruction Algorithm selected: 3D Filtered Back Projection (3DFBP)
  - Algorithm Variant: 3D Reprojection (3DRP)
    - 3D FBP algorithm which uses reprojection to fill in missing data from truncated oblique sinograms (discussed later)
- Literature survey findings: Siemens Inveon Trimodal System with NEMA NU2 Image Quality Phantom modeled and simulated using GATE
  - Reference: Sanghyeb Lee, Jens Gregor, and Dustin Osborne, "*Development and Validation of a Complete GATE Model of the Siemens Inveon Trimodal Imaging Platform*." Molecular Imaging, Decker Publishing, 2013: pp 1–13
- Reference reports use Software for Tomographic Image Reconstruction (STIR) Program with built-in 3DRP algorithm
  - Thielemans K, Tsoumpas C, Mustafovic S, et al. STIR: Software for Tomographic Image Reconstruction Release 2. Phys Med Biol, 2012;57:867–83, doi:10.1088/0031-9155/57/4/867.

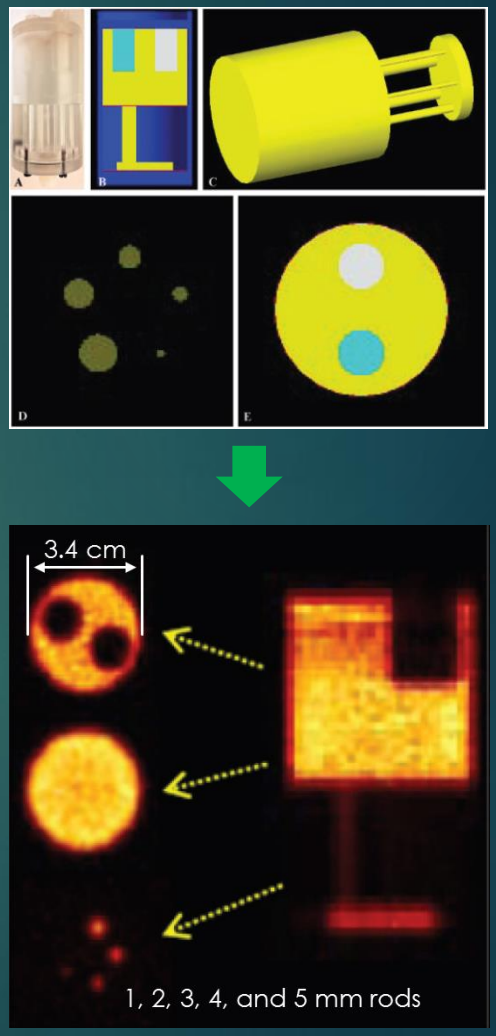

NEMA NU2 Image Quality Phantom
(GATE simulation of 10 min acquisition)

Image Reconstruction Algorithm Summary

- Prior to image reconstruction
  - LORs are acquired using detector pairs that capture coincident events
  - All corrections (e.g. for scatter, randoms and the effects of attenuation) are applied to data acquired by the PET camera,
  - The number of counts assigned to an LOR joining a pair of detectors is proportional to a line integral $p(s, \emptyset)$ of the activity along that LOR.

$$p(s, \emptyset) = \int_{-\infty}^{\infty} f(x = s \cdot \cos \emptyset - t \cdot \sin \emptyset, y = s \cdot \sin \emptyset +$$

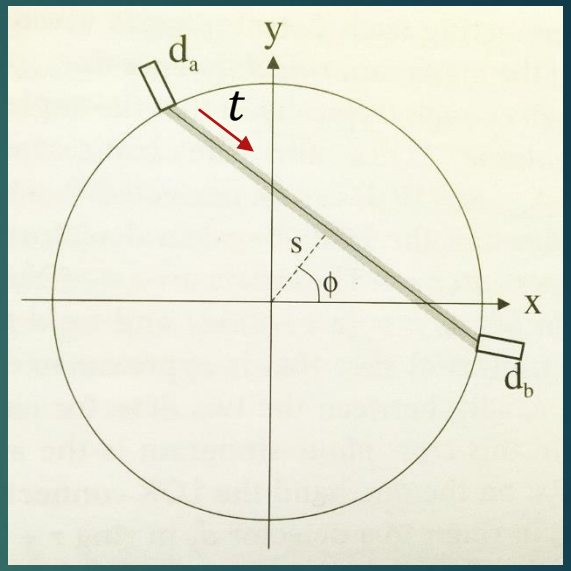

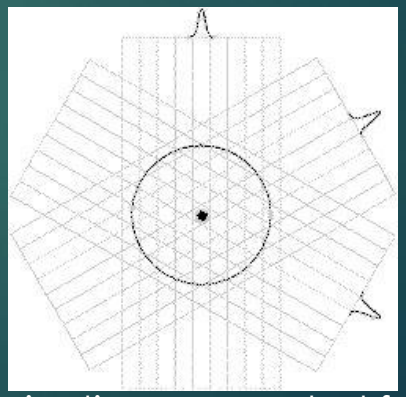

Projections generated from a single central point source (3 projections shown).

Image Reconstruction Algorithm Summary

Illustration of 2D filtered backprojection process

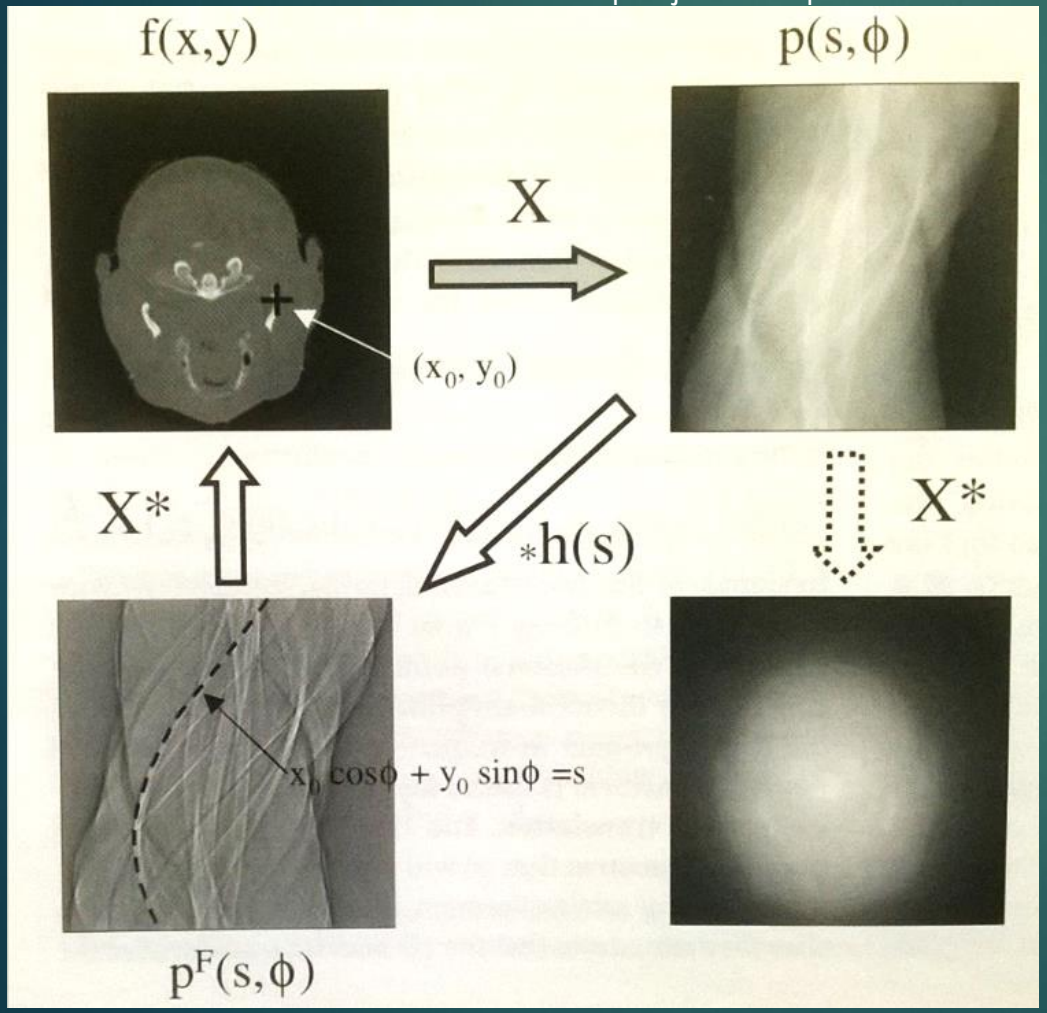

- Top row shows a physical radioisotope distribution $f(x,y)$ on the left, and its measured sinogram ($p(s,\emptyset) = Xf(x,y)$) on the right
  - X is referred to as the X-ray Transform
- Operating on sinogram with Inverse X-ray Transform (X^*p) results in unfiltered backprojection (bottom right)
  - Note blurring effect of line integral
- The filtered sinogram ($p^F(s,\emptyset)$) is obtained by 1D convolution with ramp filter kernel ($h(s)$)

$$p^F(s,\emptyset) = \int_{-R}^{R} ds' p(s',\emptyset) h(s-s')$$

where $h(s) = \int_{-\infty}^{\infty} d\nu |\nu| e^{2\pi i s \nu}$

Accomplished in frequency (ν) domain through Fourier analysis

- Inverse Xray transform on filtered sinogram (X^*p^F) results in reconstructed $f(x,y)$, Up to noise and discretization error

$$f(x,y) = (X^*p^F)(x,y)$$
$$= \int_0^{\pi} d\phi p^F(s = x\cos\phi + y\sin\phi)$$

Image Reconstruction Algorithm Summary

- 3D Implementation
  - Data from the LORs arranged into 2D sets of parallel projections (Figure 2)
  - FBP generalizes to 3D directly if the projections can be obtained over all θ as well as ϕ
    - Real cameras projections cannot easily be obtained over the full range of θ
    - Requires different filter known as the Colsher filter kernel ($h_C(\vec{s},\vec{n})$) for the convolution step

$$p^F(\vec{s},\vec{n}) = \int_{\vec{n}^\perp} d\vec{s}' p(\vec{s}',\vec{n}) h_C(\vec{s}-\vec{s}',\vec{n})$$

where $\vec{n} = (n_x, n_y, n_z) = (-\cos\theta \sin\phi, \cos\theta \cos\phi, \sin\theta)$

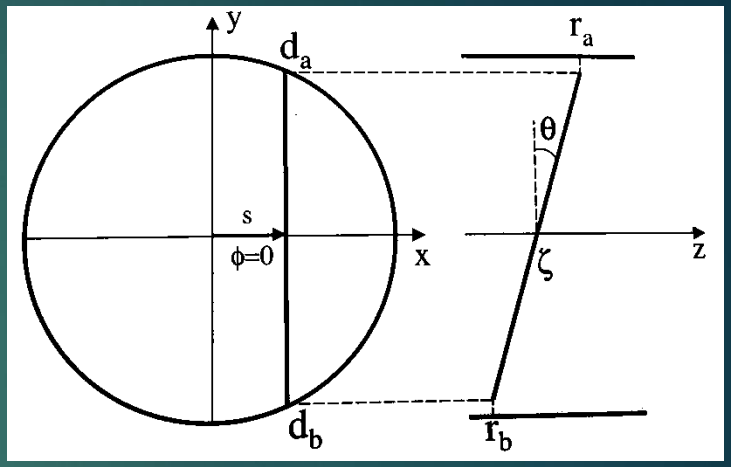

Figure 1. 3D co-ordinate system for a full-ring PET camera

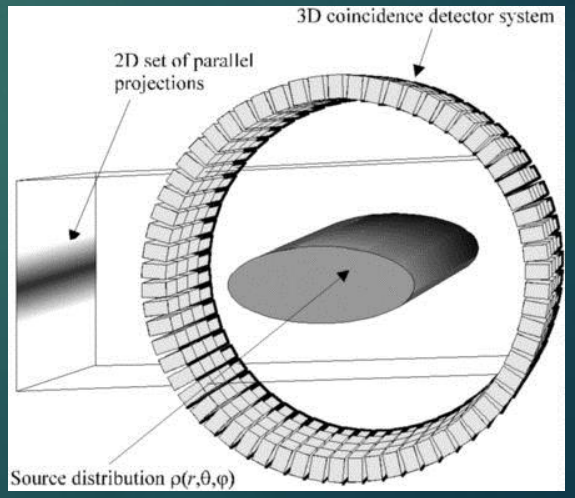

Figure 2. Parallel projections in 3D

Image Reconstruction Algorithm Summary

- 3D Reprojection used to correct for truncation in projection set
  - As θ increases, the measurable extent of the projection set decreases
  - Requires the reconstruction filter to change with position
  - To avoid this, an initial 2D reconstruction is performed on the $\theta = 0$ projection set
  - Estimates the missing parts of the truncated projections
    - Estimate obtained by reprojecting through the image volume.

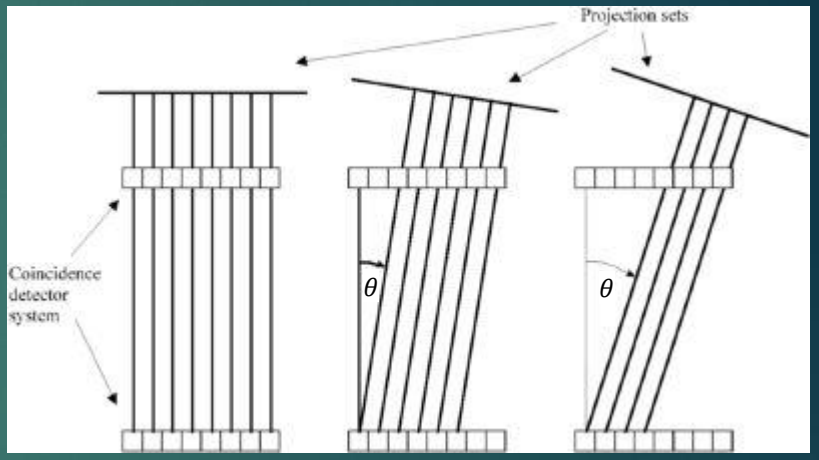

Axial cut-away diagram of a PET camera operating in 3D mode, showing the extent of the projection sets as a function of angle θ

Image Reconstruction Results

- Discrepancies found in all NEMA NU2 source reconstruction attempts
  - Highly resolved perimeter with no resolved internal features
- Found that the Ordered Subset Expectation Maximization (OSEM) algorithm has improved reconstruction over FBPRP3D
- Utilized STIR OSEM implementation –
  - No corrections to assess if cause of discrepant results are due to image reconstruction algorithm
- Results were similar – reconstruction algorithm not the cause
  - However, resolution and image quality improved.

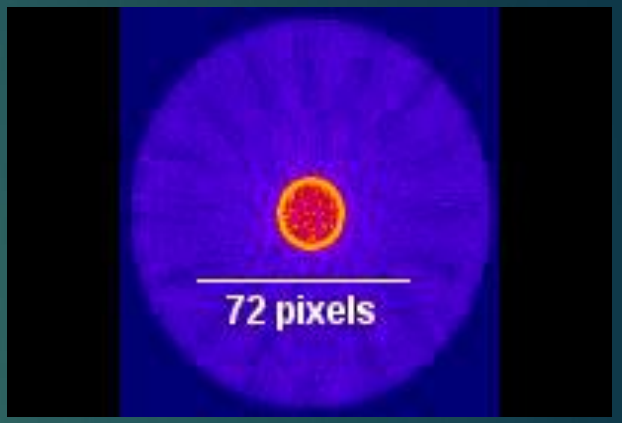

Test 05a 3D projection – 3DFBP-RP

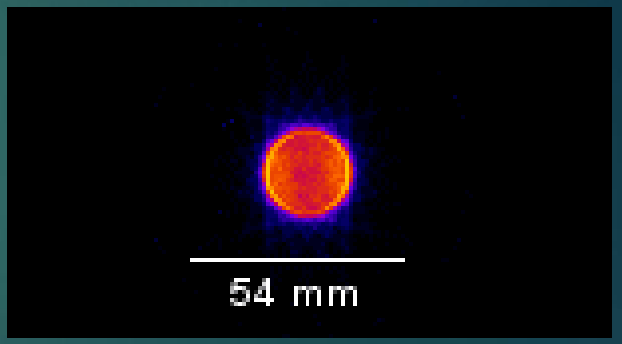

Test 05a 3D projection - OSEM

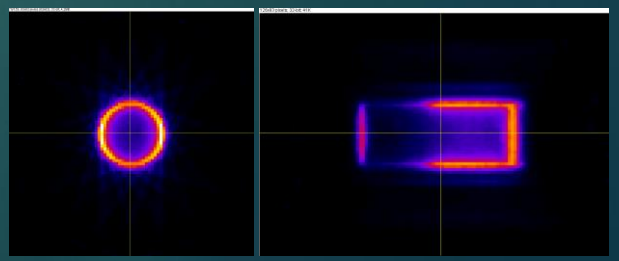

Image Reconstruction Results

- Attempted Cylindrical and Spherical source reconstruction.
  - Reconstruction not successful – no source was identifiable in either case

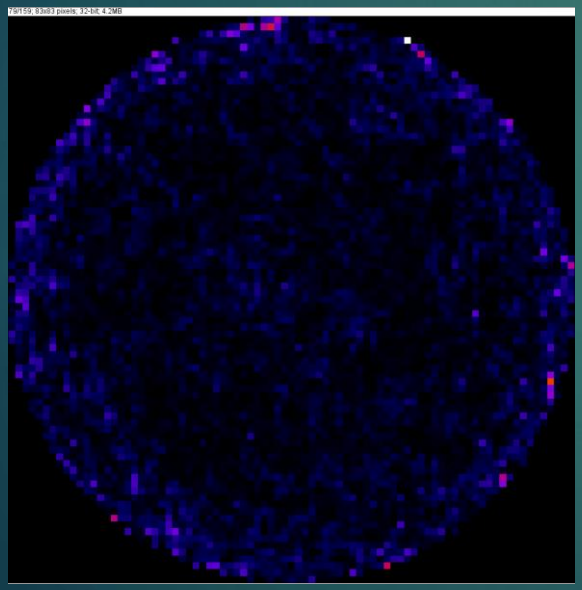

Test 01 – mid-cylinder slice

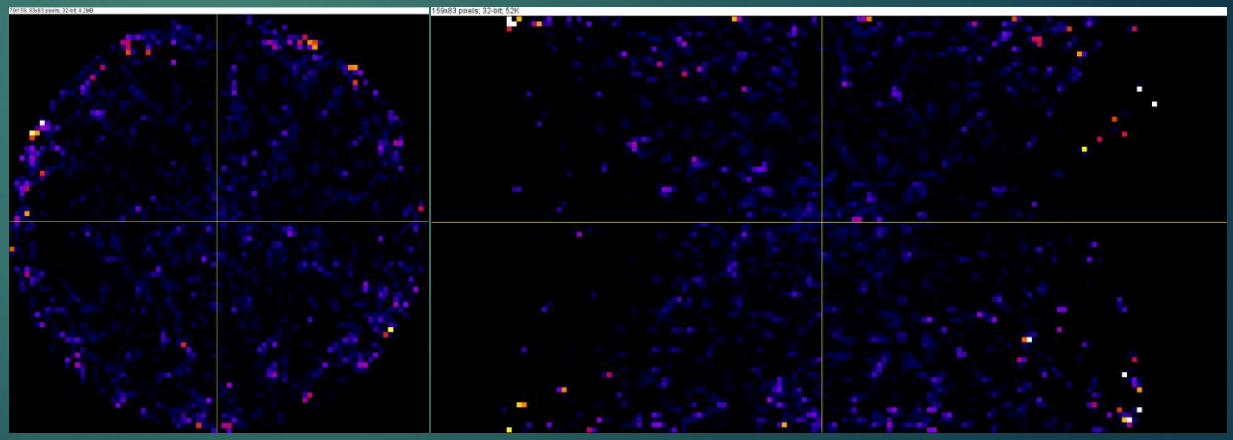

Test 05 – mid-sphere orthogonal views

Image Reconstruction Results

- Successful reconstruction of uniform cylinder was accomplished using 3DFBP-RP algorithm and sample STIR parameter input file provided in STIR installation package
- Indicating GATE-to-STIR data conversion input file not properly formatted – requires further investigation.

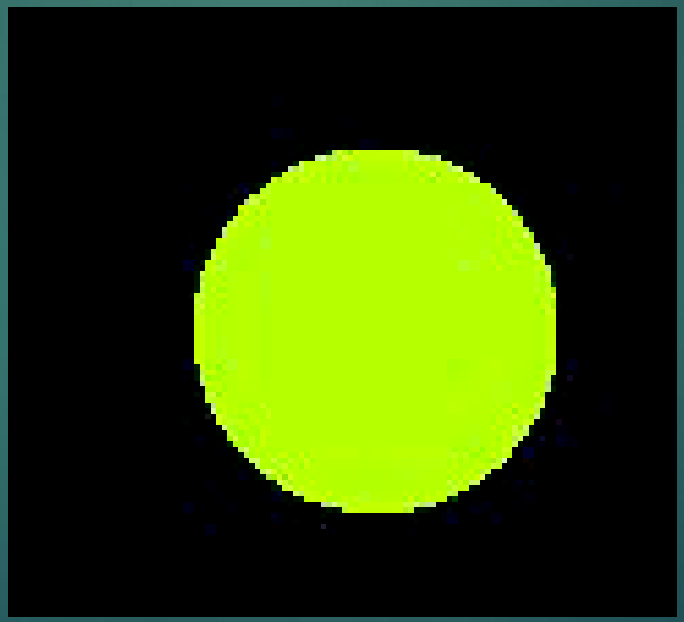

3D Projection using 3DFBP-RP algorithm and STIR Sample parameter file

Path Forward

SECTION 8

Path Forward

- Continue with CFD Simulation as previously stated
- Continue trouble shooting STIR image reconstruction output
- Generate GATE to STIR conversion script for batch processing of GATE outputs
  - Required to generate sequential, 3D projections for each time step
- Generate post-processing scripts for quantitative determination of flow feature, i.e. vena contracta, orifice diameter and axial location etc.

References

1. Stewart, P. A. E. "Neutron and Positron Techniques for Fluid Transfer System Analysis and Remote Temperature and Stress Measurement." Jounal of Engineering for Gas Turbines and Power. 110.2 (1998): 279-288. Print.
2. David Park, PEPT in engineering applications
3. Ultrafast Electron Beam X-ray Computed Tomography
4. Bailey, Dale L., et al. *Positron Emission Tomography: Basic Sciences*. London: Springer-Verlag, 2004. Print.
5. Autodesk CFD 2019 Users Manual – General Scalar Transport Equations
6. Nelson, G. and Reilly, D., "Gamma-Ray Interactions with Matter," Los Alamos National Laboratory Report, pp. 27-42
7. Sanghyeb Lee, Jens Gregor, and Dustin Osborne, "*Development and Validation of a Complete GATE Model of the Siemens Inveon Trimodal Imaging Platform*." Molecular Imaging, Decker Publishing, 2013: pp 1–13
8. Thielemans K, Tsoumpas C, Mustafovic S, et al. STIR: Software for Tomographic Image Reconstruction Release 2. Phys Med Biol, 2012;57:867–83, doi:10.1088/0031-9155/57/4/867.